Thesis for Master's Degree

Application of Compressive Sensing Theory in UWB Communication using AMP Recovery Algorithm

Hyeong ho Baek

School of Information and Communication

Gwangju Institute of Science and Technology

2013

석 사 학 위 논 문

AMP 알고리즘을 이용한 UWB 통신에서의 압축 센싱 이론의 응용

백 형 호

정 보 통 신 공 학 부

광 주 과 학 기 술 원

2 0 1 3

Application of Compressive Sensing Theory in UWB Communication using AMP Recovery Algorithm
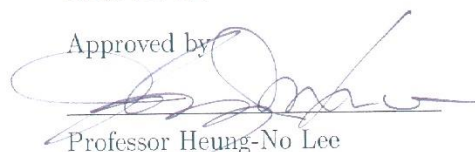
Advisor: Heung-No Lee

by

Hyeong-Ho Baek

School of Information and Communication

Gwangju Institute of Science and Technology

A thesis submitted to the faculty of the Gwangju Institute of Science and Technology in partial fulfillment of the requirements for the degree of Master of Science in the School of Information and Communication

Gwangju, Republic of Korea

2013. 12. 17.

Approved by

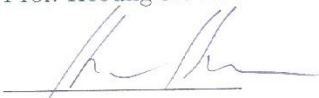Professor Heung-No Lee

Committee Chair

Application of Compressive Sensing Theory in UWB Communication using AMP Recovery Algorithm
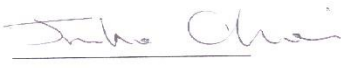
Hyeong-Ho Baek

Accepted in partial fulfillment of the requirements for the

degree of Master of Science

December 17th 2013

Committee Chair _____

Prof. Heoung-No Lee

Committee Member _____

Prof. Kiseon Kim

Committee Member _____

Prof. Jinho Choi

MS/IC   Hyeong-Ho Baek (백형호).   Application of Compressive sensing theory
20121058   in UWB communication using AMP recovery algorithm (AMP 복구 알고리즘을
          이용한 UWB 통신에서의 압축 센싱 이론의 응용). School of Information and
          Communications. 2013. 55p. Prof. Heung-No Lee

Abstract

In this paper, we introduce Approximate Message passing (AMP) algorithm which is one of the efficient recovery algorithms in Compressive Sensing (CS) [2] area. Recently, AMP algorithm [3] [4][5] has gained a lot of attention due to its good performance and yet simple structure. This paper provides not only an understanding of the AMP algorithm but its relationship with classical (Sum-Product) Message Passing (MP) algorithm. And for its application, we propose UWB channel estimation method to achieve a significant reduction of sampling rate. The proposed approach relies on the fact that the low frequencies included in the broad range of the UWB frequency spectrum have a long wavelength, which allows UWB signal to penetrate a variety of materials. This means there are few multi-paths with sufficient high power, yielding thus a sparse representation of the channel impulse response. And the received waveforms can be modeled as result from convolution of very short pulse and impulse response of channel. Thus, the transformation matrix is designed as convolution matrix. Meanwhile, reconstruction algorithms which are computationally expensive and complex are not suitable for real time application like UWB communication. Because of this reason, we used the Approximate Message Passing algorithm which has shown to achieve very good performance with large reduction on complexity in comparison with existing approaches to estimate the channel impulse response. Lastly, we applied the proposed estimation method based compressive sensing to a Rake receiver. Actually, a Rake receiver must know the time distribution for all multi-path contributions composing the received waveform and the knowledge of the amplitudes of the

multi-path components is also required for exploiting diversity. In simulation, we compare performances of the UWB channel estimation by changing the recovery algorithms; L1 norm, IST [6] , AMP, MP [7]. The results show AMP algorithm has computationally simple structure and good recovery performance. Thus, the algorithm is suitable for UWB channel estimation.

Contents

List of Figures

List of Tables

1 Introduction of Compressive Sensing

1.1 Compressive sensing

The existing information and communication system has developed by digital system based Shannaon and Nyquist Sampling theorem. The digital system is starting from changing natural analog signal to digital signal. Once the analog signal like image and voice is changed, we can express this signal as integer number not real number. So we can store, copy and convey the signal using the computer.

The first step of changing the natural signal to digital signal is performed by Analog to Digital Converter (ADC). Therefore ADC is the basic essential in the everywhere Digital system is used. Such ADC is made based Shannon-Nyquist sampling theory. And according to the appearance of small transistor technology, ADC becomes more and more highly integrated. This means ADC has evolved several different times to operating faster and lower power. By the way, sampling rate of ADC is in proportion to the quantity of information can be expressed. Correctly speaking, the sampling rate must be twice the maximum frequency present in the signal in order to perfectly recover the signal. The theory has used by basis theory to construct digital system up to this day.

The Shannon-Nyquist sampling theory is reviewed by academia. This chapter will examine this recent trend.

The Compressive Sensing (CS) was introduced by Donoho, Candes, and Tao at IEEE Transaction on Information Theory. CS theory in this chapter limits the thing which made by these authors. The interesting thing that this theory suggests is to perfectly recover the signal using far fewer samples of measurements than traditional methods. CS allows to compress the data while is sampled. As explained in [1][8][9] most of the signals can be represented by sparse. It means when the signal is drew at $x-y$ graph, most of x match up with zero y and a good few x match up with non-zero y. According to the CS theory, the sparse signal can be perfectly recovered from far fewer linear measurements is a central idea. More accurate number of linear measurements is about $O(K\log(N/K))$ where K is non-zero entries and called as 'sparsity'. And N is the length of signal.

1.2　Review of Compressed Sensing Theory

We can reduce the center of CS theory is to find solution of following equation:

$$\mathbf{y} = \mathbf{A}\mathbf{x} \tag{1}$$

where $\mathbf{x}$ is original sparse signal of dimension $N \times 1$, $\mathbf{A}$ is $M \times N$ dimensional matrix, called as the Sensing matrix, representing the linear combinations of compressed sensing and $\mathbf{y}$ is the vector of resultant samples of size $M \times 1$ commonly referred to as measurements and M is smaller than N. Thus this equation is to solve under determined system. Meanwhile, Sparsity is defined as the number of non-zero value of original signal and expresses K. The relation of M, N, K is $K < M \ll N$.

If the signal $\mathbf{x}$ is not sparse signal, it can be made sparse by transforming to any suitable bases such as fourier, wavelets etc. and it has been observed that most naturally occurring signals are sparse in some suitable bases.

Consider the following real-valued, finite length, discrete time signal $\mathbf{x} \in \mathbb{R}^N$ which can be expressed in an orthonormal basis $\mathbf{\Psi} = [\psi_1 \quad \psi_2 \quad \cdots \quad \psi_M]$ as follows:

$$\mathbf{x} = \sum_{i=1}^{M} \psi_i \theta_i \tag{2}$$

where the vector $\mathbf{\theta} = [\theta_1 \quad \theta_2 \quad \cdots \quad \theta_N]$ is a sparse vector, which means that is a vector with very few non-zero components. Using matrix notation it may be presented as

$$\mathbf{x} = \mathbf{\Psi}\mathbf{\theta} \tag{3}$$

where matrix $\mathbf{\Psi}$ had dimension $N \times N$. A vector with only K non-zero components is called K-sparse vector in that particular basis. To apply equation (3), we can represent equation (1) as follow.

$$\mathbf{y} = \mathbf{Ax} = \mathbf{\Phi\Psi\theta} \tag{4}$$

where $\mathbf{\Phi\Psi}$ form the effective measurement matrix for estimating the $K-sparse$ vector $\mathbf{\theta}$. Matrix $\mathbf{A}$ is called measurement matrix and it has rank M lesser than the rank of the signal $\mathbf{x}$ which is equal to N. The $M \times N$ matrix $\mathbf{A}$ is projecting the signal $\mathbf{x}$.

$y \in R^{M \times 1}$
Measurement

$\mathbf{A} \in R^{M \times N}$

$\Psi \in R^{N \times N}$

$x \in R^{N \times 1}$
K(nonzero entries)
-Sparse signal
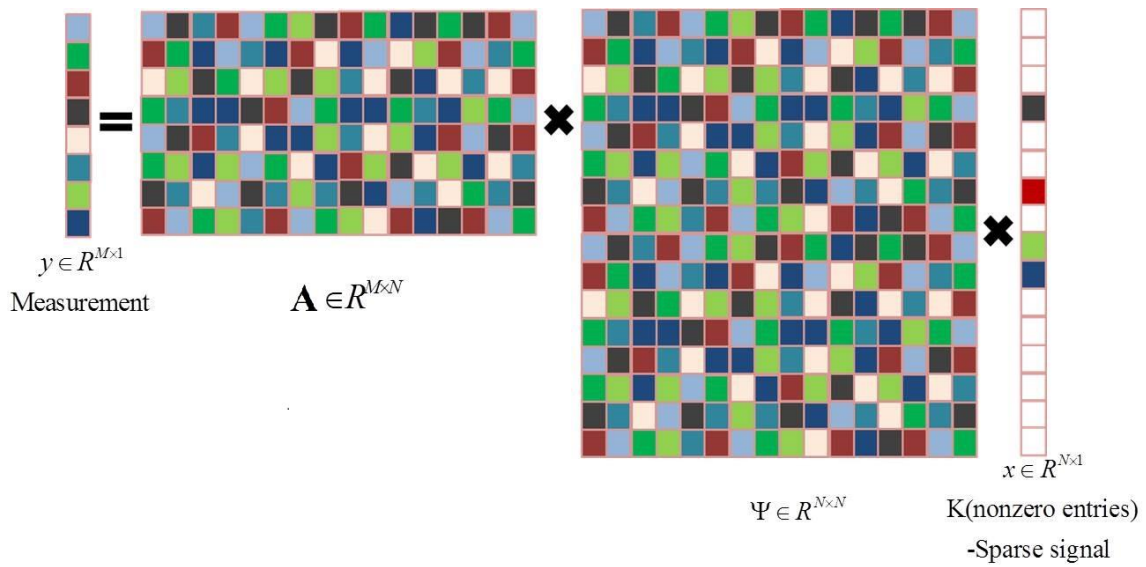
Figure 1 Brief expression of Compressed Sensing

1.2.1 The Sensing Matrix $\mathbf{A}$ and RIP Condition

In this section we will explain how to make or find sensing matrix $\mathbf{A}$. Candes, Romberg and Tao [8][9] used Gaussian, Bernoulli distribution matrix or Fourier matrix. When that times, the recovery probability is high using $O(K\log(N/K))$ samples of measurements. And the matrix set consists of these matrices has high probability of satisfying Restricted Isometric Property (RIP). RIP can be represented by following equation.

$$(1-\gamma)\|\mathbf{x}\|_2 \leq \|\mathbf{Ax}\|_2 \leq (1+\gamma)\|\mathbf{x}\|_2 \tag{5}$$

where $0 < \gamma < 1$ is constant called as RIP Constant. Summarized this RIP condition, it means sensing matrix $\mathbf{A}$ has to project uniform energy onto sparse signal $\mathbf{x}$. The length of measured vector $\mathbf{y}$ is equal to the length of $\mathbf{x}$. The important thing is length has to equal even though any signal $\mathbf{x}$ is used.

If sensing matrix $\mathbf{A}$ projects onto signal $\mathbf{x}$ in specific subspace, it means there is subspace where the matrix cannot project well. And then if the signal $\mathbf{x}$ is on subspace where preference region, the recovery performance is good. However the inverse case, the chances of an error occurring in recovery increase. Thus, in order to cover the signal on the entire region the sensing matrix $\mathbf{A}$ which projects uniform energy onto any vector $\mathbf{x}$ is most suitable sensing matrix. However to conform any sparse signal satisfy RIP condition is NP-hard problem. It means we have to examine the entire probable case. Thus using equation (5) is not good method to measure the sensing matrix is good or not. We will propose practical method in section 1.5.

1.2.2 CS Recovery Criteria

As mentioned earlier, equation (1) is under determined system. Thus equation (1) has numberless solutions. This can be explained using null space of sensing matrix $\mathbf{A}$ in the following manner. Actually, the $\mathbf{x}+\mathbf{u}$ is also solution where $\mathbf{x}$ is signal and $\mathbf{u}$ is entire vector in the null space. That

is $\mathbf{y} = \mathbf{A}(\mathbf{x} + \mathbf{u})$. However, because we want to find sparse solution, we need to find most sparsest solution among $\mathbf{x} + \mathbf{u}$. Below, we will present three kinds of methods to solve equation (1) and explain each characteristics briefly.

- Minimum L2 norm reconstruction :

$$\overline{\mathbf{x}} = \arg\min \| \mathbf{x} \|_1 \text{ such that } \mathbf{Ax} = \mathbf{y} \tag{6}$$

The solution of this optimal problem is widely known as $\overline{\mathbf{x}} = \mathbf{A}^T (\mathbf{AA}^T)^{-1} \mathbf{y}$. But this method is not suitable to find sparse solution. Because the solution of minimum L2 norm reconstruction is non spare which has a lot of non-zero value, the solution is much different from real solution.

- Minimum L0 norm reconstruction: Using L0 norm $\| \mathbf{x} \|_0$ which presents the number of non-zero to the optimal problem, we can make the best use of sparse characteristic. In order words, minimum L0 norm reconstruction can be represented by following equation.

$$\overline{\mathbf{x}} = \arg\min \| \mathbf{x} \|_0 \text{ such that } \mathbf{Ax} = \mathbf{y} \tag{7}$$

At this moment if the number of measurements is $M \geq 2K$, we can get K-sparse signal. But Equation (7) is NP-hard problem to check $\binom{N}{K}$ K-sparse vector. So, this method lacks practicality.

- Minimum L1 norm reconstruction:

$$\overline{\mathbf{x}} = \arg\min \|\mathbf{x}\|_1 \text{ such that } \mathbf{Ax} = \mathbf{y} \tag{8}$$

The L1 norm of vector $\mathbf{x}$ defines sum of the entire absolute elements.
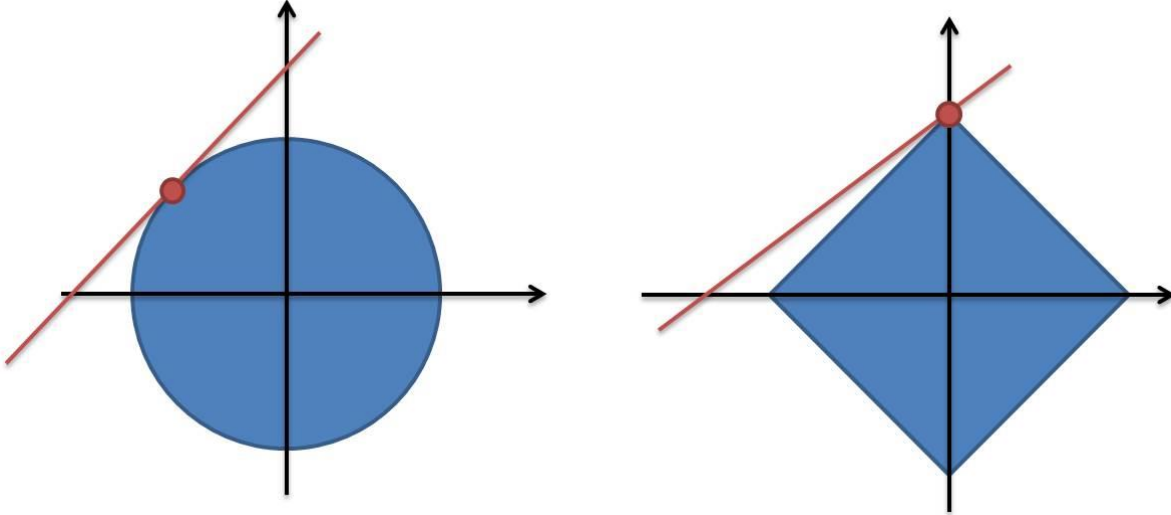
Figure 2 Geometry of l_2, l_1 recovery

Using minimum L1 norm reconstruction, K-sprase signal is likely to be recovered using only $M \geq ck\log(N/K)$ measurement values [8][9]. We can solve this optimization problem to transpose linear problem called as Basis Pursuit [10]. And the computational complexity of this is about $O(N^3)$.

The Figure 2 expresses geometry of minimum L1 norm reconstruction and minimum L2 norm reconstruction. To visualize how minimum L2 norm reconstruction accomplishes, imagine taking an L2 ball of tiny radius and gradually expanding it until it intersects with the solution line for the first time. In the same way, we can visualize how to minimum L1 norm reconstruction accomplishes. The specific thing is L1 ball is diamond-shaped.

Let's compare the solution of minimum L1 norm reconstruction with the solution of minimum L2 norm reconstruction. As Figure 2, the solution of minimum L2 norm reconstruction is not sparse. On the other hand, the solution of minimum L1 norm reconstruction is sparse. Thus, the minimum L1 norm reconstruction finds proper solution of CS problems.

1.2.3 Condition for Unique Solution

As mentioned earlier, we explained minimum L1 reconstruction finds the sparse solution. Thus, this method is likely to find the solution of CS problems. In this section, Let's look into what conditions are for the solution of minimum L1 reconstruction to be the unique one and the unique one to be in accord with the solution of minimum L0 reconstruction. This conditions are closely related with sensing matrix $\mathbf{A}$. In order word, sensing matrix $\mathbf{A}$ satisfies RIP condition. However, this is NP-hard problem and so we will suggest another method. The method is to check Coherence of $\mathbf{A}$.

- Maximum coherence of $\mathbf{A}$: Let the column of matrix $\mathbf{A}$ is $i = 1, 2, \cdots, N$, and each column is normalized. In that time, maximum coherence of $\mathbf{A}$ defines as following equation.

$$\mu(\mathbf{A}) := \max_{i \neq j} \left| \left\langle \mathbf{a}_i, \mathbf{a}_j \right\rangle \right| \tag{9}$$

Sensing matrix $\mathbf{A}$ is closely related with recovered solution. This being so, Maximum coherence is also closely related. We already knew that there are no end of solutions is satisfied equation (1). However, we need to get sparsest solution among these solutions. Donoho and Huo express the necessary condition of to get unique solution as maximum coherence in [11].

- Condition that the solution of minimum L0 reconstruction is unique one : The signal is K-sparse and to get unique solution using minimum L0 reconstruction, the following condition is satisfied [11].

$$\|\mathbf{x}\|_0 < \frac{1}{\mu(\mathbf{A})} \tag{10}$$

Let us we compare sensing matrices with same dimension $[M \times N]$. If the maximum coherence of $\mathbf{A}$ become smaller then, we can recover high sparsity signal. This means the more the maximum coherence of $\mathbf{A}$ become smaller, the sensing matrix $\mathbf{A}$ is better.

- Condition that the solutions of minimum L0 and L1 reconstruction are same: If we use sensing matrix which satisfies equation (10), the solution of minimum L0 reconstruction is unique. However, this condition does not guarantee the solutions of minimum L0 and L1 reconstruction are same in the minimum L1 reconstruction case. Thus to do this, we need strict condition as follow.

$$\|\mathbf{x}\|_0 \leq \frac{1}{2}\left(1 + \frac{1}{\mu(\mathbf{A})}\right) \tag{11}$$

Now we consider about low bound of maximum coherence value. In other word, when the dimension of sensing matrix is $[M \times N]$, let us try to express the low bound of maximum coherence as the equation to M and N. If it is possible, we can know the relationship between sparsity $\|\mathbf{x}\|_0$ and M, N i.e. we can know the maximum sparsity level of solution that is obtained by minimum L1 reconstruction from M, N.

- Low bound of maximum coherence : Let dimension of sensing matrix $\mathbf{A}$ is $M \times N$. And then low bound of $\mu(\mathbf{A})$ is follow.

$$\mu(\mathbf{A}) \geq \sqrt{\frac{N - M}{M(N - 1)}} \tag{12}$$

This means the more M is increased, $\mu(\mathbf{A})$ is the more close to zero.

1.3 Stable Recovery

Now we consider about performance of minimum L1 reconstruction in practical situation. In practical situation, the signal is added noise. And we need to consider the target signal is not K-sparse . First, let us talk about performance of minimum L1 reconstruction in noise environment.

In noise environment, minimum L1 reconstruction for recovering signal is changed following equation.

$$\overline{\mathbf{x}} = \arg\min \| \mathbf{x} \|_1 \text{ such that } \| \mathbf{A}\mathbf{x} = \mathbf{y} \|_2 \leq \varepsilon \tag{13}$$

where $\mathbf{y} = \mathbf{A}\mathbf{x} + \mathbf{e}$ and $\| e \|_2 \leq \varepsilon$. In this case, Candes said the square of absolute value of recovery error is less than or equals to constant multiplication of noise energy. If the number of non-zero element of signal $\mathbf{x}$ is less than or equals to K and energy of noise vector $\mathbf{e}$ is less than ε, following equation is satisfied.

$$\left\| \mathbf{x}^* - \mathbf{x}_0 \right\|_2 \leq C\varepsilon \tag{14}$$

where $\mathbf{x}^*$ is solution of equation (13). This means if the signal is added noise, it is possible to reconstruct the original signal using minimum L1 reconstruction.

Next let us talk about performance of minimum L1 reconstruction when the target signal is not K-sparse . Basically, after assuming the target signal is not K-sparse , minimum L1 reconstruction is performed. Thus recovery error is remained signal energy except K number of largest values.

If the number of non-zero element of signal $\mathbf{x}$ is less than or equals to K and energy of noise vector $\mathbf{e}$ is less than ε, following equation is satisfied.

$$\left\| \mathbf{x}^{*} - \mathbf{x} \right\|_{2} \leq C_{1}\varepsilon + C_{2}\frac{\left\| \mathbf{x} - \mathbf{x}_{K} \right\|}{\sqrt{K}} \tag{15}$$

where $\mathbf{x}_{K}$ is K-sparse signal. This equation means the magnitude of recovery error is not much different with modeling error $\left\| \mathbf{x} - \mathbf{x}_{K} \right\|_{1}$.

1.4 Summary

Until now we looked into Compressive sensing. Briefly speaking, Compressive sensing is new signal acquisition or recovery method that is compressed and sampled compressible signal in acquisition step. Donoho emphasized the superiority of Compressive sensing in [26]. And Shannon-Nyquist sampling theory gives pressure to get a lot of samples to reconstruction original signal. His opinion is not something we can just pass over. Thus, we reviewed Compressive sensing theory that Donoho and Candes, Tao [1][8][9] published in this chapter.

2 Ultra Wideband Communications Overview

2.1 Introduction

The recent steady growth in technology and the commercial deployment of wireless communications are considerable affecting our daily lives. The transition from analog to digital communications are enabling consumers to access a wide range of information from anywhere and at any time. As the consumer demand for higher capacity, faster service, and more secure wireless communication increases, new advanced technologies have to find empty spectrum in the overcrowded spectrum. This is because every radio technology allocates a specific part of the spectrum; for example, the signals for TVs, radios, cell phones, and so on are sent on different frequencies to avoid interference to each other. As a result, the focus of new communication technology is concentrated as the new radio services.

Ultra-wideband (UWB) technology offers an expectable solution to the RF spectrum exhaustion by allowing new services to coexist with current radio systems with minimal or no interference. This coexistence brings the advantage of avoiding the expensive spectrum licensing cost. This chapter provides a comprehensive overview of ultra-wideband communications, starting with its history and background.

2.2 History and Background

Ultra-wideband communications is basically different from all other communication techniques because it employs extremely narrow pulses signal to communicate between transmitters and receivers. Utilizing short-duration pulses for communications directly generates a very wide bandwidth and offers several advantages, such as large throughput, covertness, robustness to jamming, and coexistence with current radio services.

Ultra-wideband communications is not a new technology. In fact, it was first employed by Guglielmo Marconi in 1901 to transmit Morse code across the Atlantic Ocean using spark gap radio transmitters. However, the benefit of a large bandwidth and the capability of implementing multiuser systems provided by electromagnetic pulses were never considered at that time.

Approximately fifty years after Marconi, modern pulse-based transmission used in military applications in the form of impulse radars. Some of the pathfinder of modern UWB communications in the United States from the late 1960s are Henning Harmuth of Catholic University of America and Gerald Ross and K. W. Robins of Sperry Rand Corporation. From the 1960s to the 1990s, this technology was restricted to military and Department of Defense applications under classified programs such as highly secure communications. However, the recent advancement in microprocessing and fast switching in semiconductor technology has made UWB ready for commercial applications. Therefore, it is more appropriate to consider UWB as a new communication technology.

In February 2002, the Federal Communications Commission approved the First Report and Order for commercial use of UWB technology under strict power emission limits for various devices..

2.3   UWB Concepts

Traditional narrowband communications systems modulate continuous waveform signals with a specific carrier frequency to transmit and receive information. A continuous waveform has defined signal energy in a narrow frequency band that makes it very prone to detection and interception.

As mentioned UWB systems use carrierless, short-duration pulses with a very low duty cycle for transmission and reception of the information. Simple definitions for duty cycle is the ratio of the time that a pulse is present to the total transmission time as following equation and describe Figure 3.
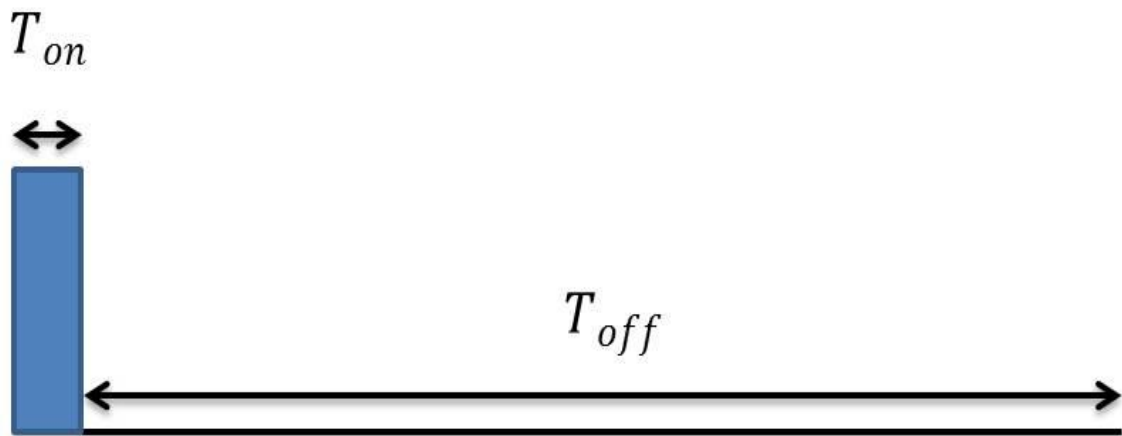
Figure 3 A low duty cycle pulse. T_{on} **is the time that the pulse exists and** T_{off} **is the time that the pulse is absent.**

$$\text{Duty Cycle} = \frac{T_{on}}{T_{on} + T_{off}} \qquad (16)$$

Low duty cycle offers a very low average transmission power in UWB communications systems. The average transmission power of a UWB system is on the order of microwatts. However, instantaneous power of individual UWB pulses can be relatively large. But because they are transmitted for only a very short time, the average power becomes considerably lower. Consequently, UWB devices require low transmit, which directly leads the longer battery life. Since frequency is inversely related to time, the short-duration UWB pulses spread their energy across a wide range of frequencies from near DC to several GHz with very low power spectral density (PSD). Figure 4 and 5 illustrates UWB pulses in time and frequency domains.
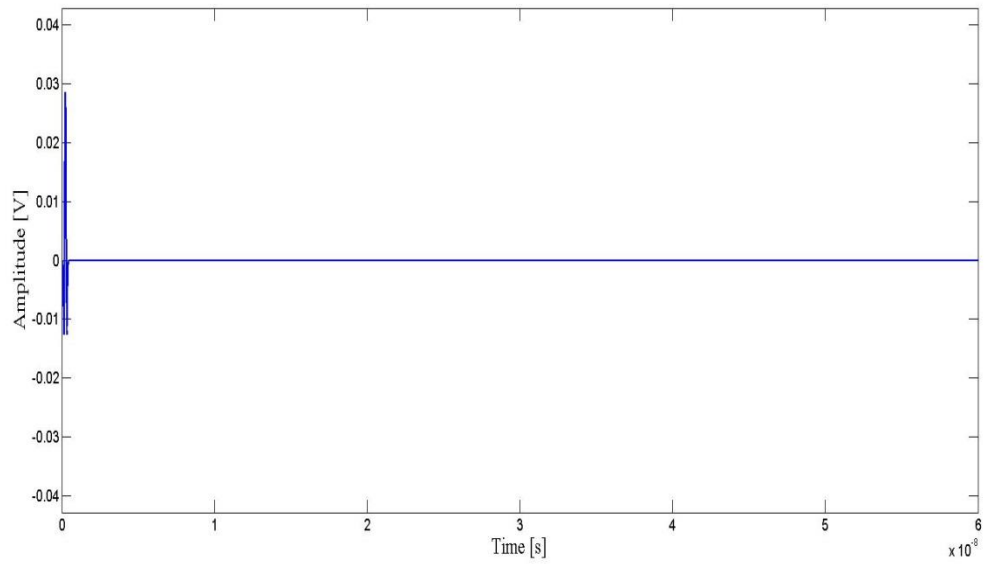
Figure 4 A UWB pulse in the time domain
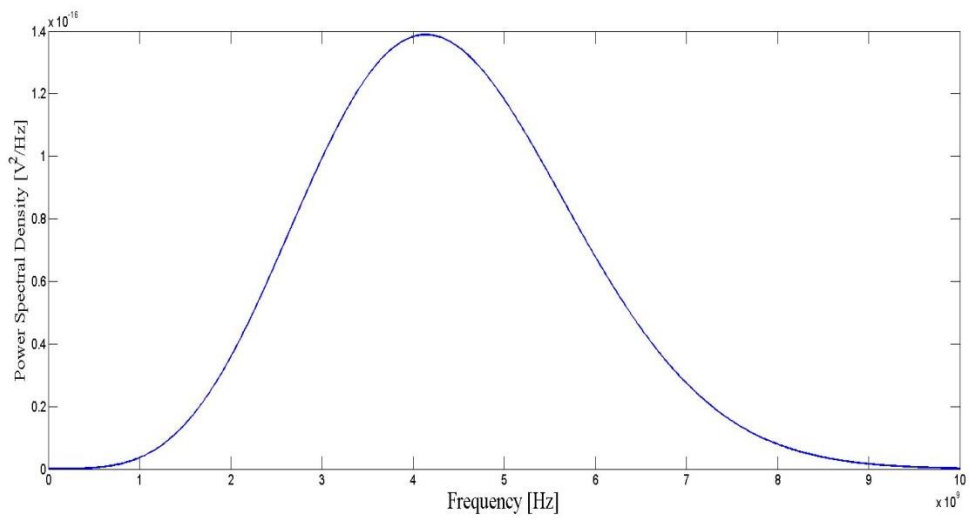
Figure 5 A UWB pulse in the frequency domain.

2.4 UWB Signals

As defined by the Federal Communications Commission, UWB signals have to have bandwidths of greater than a fractional bandwidth larger than 20 percent at all times of transmission. To better understand this definition, we first need to define the energy bandwidth of the waveform. If E is the instantaneous energy of the waveform, the energy bandwidth is then identified by the frequencies f_L and f_H, which delimit the interval where most of E falls. We call the width of the interval $[f_L, f_H]$ is the energy bandwidth.

A UWB signal can be any one of a variety of wideband signals, such as Gaussian, chirp, wavelet based short-duration pulses.

Classification of signal	Fractional bandwidth (B_f)
Narrowband	$B_f < 1\%$
Wideband	$1\% < B_f < 20\%$
Ultra-Wideband	$B_f > 20\%$

Figure 6 The classification of signal based on fractional bandwidth

2.5 Advantages of UWB Signals

As defined by the Federal Communications Commission, UWB signals have to have bandwidths of greater than a fractional. In this subsection, we will show some of the benefits that UWB brings to wireless communications.

2.5.1 Possible to share the Frequency spectrum

The power restriction by Federal Communications Commission for UWB systems allows UWB systems to reside below the noise floor of a typical narrowband receiver and enables UWB signals to coexist with current radio services with minimal or no interference. However, this all depends on the type of modulation used for data transfer in a UWB system.
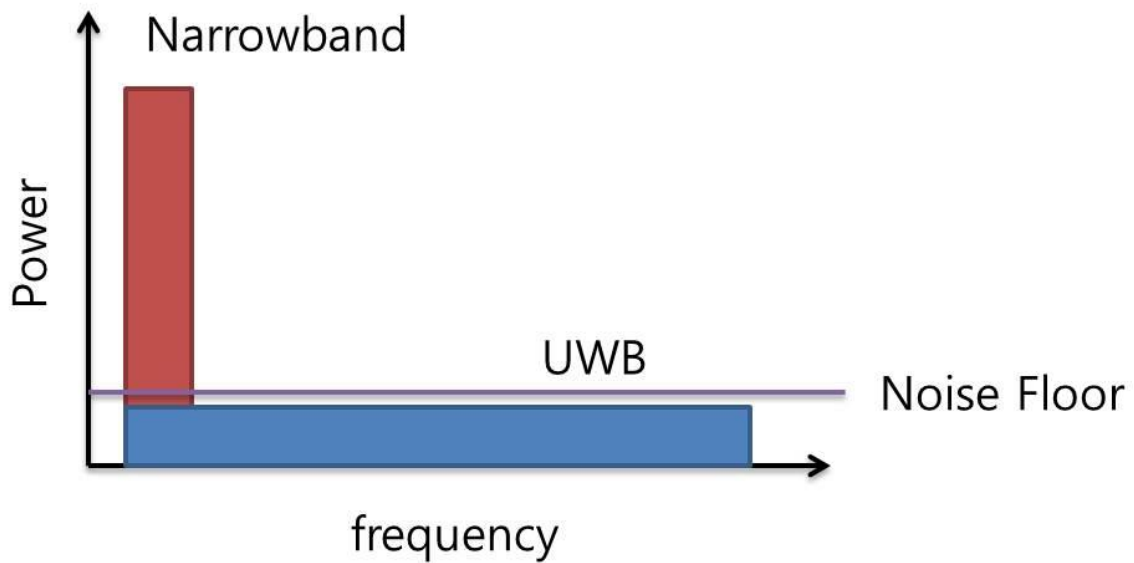
Figure 7 Coexistence of UWB signals with narrowband in the spectrum

2.5.2 High Channel Capacity and Ability to work with low SNR

One of the major benefits of the large bandwidth for UWB pulses is improved channel capacity. Channel capacity is defined as the maximum amount of data that can be transmitted per second over a communications channel. This fact is proved by Shaanon's capacity formula.

$$C = B \log_2(1 + SNR) \tag{17}$$

where C is the maximum channel capacity, B is the bandwidth. As shown equation (17), channel capacity C linearly increases with bandwidth B. Hence, having several GHz of bandwidth available for UWB signals, a data rate of Gbps can be expected. And UWB communications systems are capable of working in communication channels with low SNR and still offer a large channel capacity as a result of their large bandwidth.

2.5.3 Low probability of Intercept and Detection and Resistance to Jamming

Because of their low average transmission power, UWB communication systems have immunity to detection and intercept. In addition, UWB pulses are time modulated with codes unique to each transmitter and receiver pair. The time modulation of extremely narrow pulses adds more security to UWB transmission, because detecting picosecond pulses without knowing when they will arrive is next to impossible. And if some of the frequencies are jammed, there is still a large range of frequencies that remains untouched. Hence, the UWB communication system have resistance to Jamming.

2.5.4 High Performance in Multipath Channel

The multipath is unavoidable in wireless communications channels. It is caused by multiple reflections of the transmitted signal from various surfaces. However, the very short duration of UWB pulses makes less sensitive to the multipath effect. Because the transmission duration of a UWB pulse is shorter than a nanosecond in most case, the reflected pulse has an extremely short window of opportunity to collide with the reflected pulses.

2.5.5 Superior Penetration Properties and Simple Transceiver Architecture

UWB systems can penetrate effectively through different materials. The low frequencies included in the broad range of the UWB frequency spectrum have a long wavelength, which allows UWB signals to penetrate a variety of materials. And UWB transmission is carrierless, meaning that data is not

modulated on a specific carrier frequency wave, as in narrowband and wideband technologies. For this reason UWB transceiver architecture is significantly simpler and cheaper to build.

2.6   Challenges

There are many challenges involved in using UWB communications.

2.6.1 Pulse-shape Distortion

The transmission characteristics of UWB pulses are more complicated than those of continuous narrowband sinusoids. The low powered UWB pulses can be distorted significantly by the channel. This will limit the performance of UWB receivers that correlate the received pulses with a predefined template.

2.6.2 Channel Estimation

Channel estimation is a central issue for receiver design in wireless communications systems. Given that most UWB receivers correlate the received signal with a predefined template signal, prior knowledge of the wireless channel parameters is necessary to predict the shape of the template signal that matches the received signal. However, as a result of the wide bandwidth and reduced signal energy, channel estimation in UWB communications systems becomes very complicated

2.6.3 Time Synchronization

Time synchronization is another major in UWB communications systems. As with any other wireless communications system, time synchronization between the receiver and the transmitter is a must for UWB pairs. However, sampling and synchronizing nanosecond pulses place a major limitation on the

design of UWB systems. In order to sample these narrow pulses, very fast analog-to-digital converters

(ADC) are needed.

3 Introduction and Performance Analysis of Approximate Message Passing (AMP) for Compressed Sensing Signal Recovery

3.1 Abstract

In this section, we introduce Approximate Message Passing (AMP) algorithm which is one of the efficient recovery algorithms in Compressive Sensing (CS) [1] area. Recently, AMP algorithm has gained a lot of attention due to its good performance and yet simple structure. This paper provides not only a understanding of the AMP algorithm but its relationship with a classical (Sum-Product) Message Passing (MP) algorithm. Numerical experiments show that the AMP algorithm outperforms the classical MP algorithms in terms of time and phase transition.

3.2 The appearance of Compressive Sensing and Object

The first step to convert a continuous-time analog signal to a discrete-time digital signal is to discretize the signal in time, which is called sampling. A common approach in engineering is to assume that the signal is bandlimited, meaning that the spectral contents are confined to a maximal frequency $f_{\max}$. Bandlimited signals have limited time variation, and can therefore be perfectly reconstructed from samples with a rate at least $2f_{\max}$, termed the Nyquist rate. This fundamental result is often attributed in the engineering community to Shannon-Nyquist. However, researchers in image, video, and audio processing observed that the Shannon-Nyquist sampling is not efficient or optimal and asked following question. "Is it possible to adjust the sampling rate according to information quantity that the signal contains?" Compressive Sensing (CS) which Candes and Donoho has been proposed replied to the question. "If the target signal is sparse sufficiently, it is possible to

acquire all of information about this signal without having a performance loss using M samples which is smaller than the signal length N."

The CS theory in the introduction above and classical Nyquist sampling theory differ in the structure of signal acquisition basically. In Nyquist, the signals were first sampled at a high sample rate to preserve desired signal information and then secondly some compression algorithm was performed to reduce the resultant large number of samples from the first step, in order to reduce the complexity and cost of the subsequent image processing and storage. Namely, "sample and compress". On the other hand, it is possible to replace the two steps of high-rate sampling and compression with a single step in CS theory. Namely, "compression on the fly".

However, the apparent defiance of the Nyquist sampling criterion in compressed-rate sampling is possible only under two special requirement: 1) The presence of more sophisticated and intelligent sampling scheme than the one present in the above mentioned two step process and 2) the signal to be acquired must be a sparse signal. If our target signal is not sparse, it can be made sparse by compressing it in any suitable bases [24]. For example, a signal is dense in time domain, but the signal is sparse in frequency domain. Thus, second requirement can be solved by finding suitable bases.

In CS, linearly projecting target signal into any sensing matrix describe "compression on the fly". And phenomenon of this acquisition process of CS can then be efficiently represented as the following equation.

$$\mathbf{y}_{(M\times 1)} = \mathbf{A}_{(M\times N)}\mathbf{s}_{(N\times 1)} \tag{18}$$

where $\mathbf{s}$ is our target sparse signal of dimension $N\times 1$ which we want to compressively acquire. And $\mathbf{A}$ is an $M\times N$ dimensional matrix, called as the Sensing matrix, representing the linear combinations of compressed sensing and $\mathbf{y}$ is the vector of resultant samples of size $M\times 1$ commonly referred to as measurements. A large number of recovery algorithms have also been proposed in literature having their origins in diverse fields and areas e.g. convex optimization [23],

linear programming [1], bases decomposition [13], combinatorial methods, iterative shrinkage, graphical models [12] etc. One such recovery algorithm recently proposed by Maleki and Donoho and known as the Approximate Message Passing (AMP) algorithm has shown to achieve very good performance with large reduction on complexity in comparison with existing approaches. Unfortunately, although the AMP algorithm can be applied to various fields, papers to introduce AMP are inadequate. Thus, guidelines to help to understand AMP algorithm and to apply can play an important role. This chapter provides not only an understanding of the AMP algorithm but its relationship with a classical Sum-product Message Passing (MP) algorithm. Numerical experiments and characteristic of AMP show that the AMP algorithm outperforms.

3.3   Derivation of AMP algorithm

3.3.1 Derivation of AMP from classical Sum-Product MP Algorithm

The first step to convert a continuous-time analog signal to a discrete-time digital signal is to discretize we explain the notation that will be used throughout the paper and define factor graph and message that are used in MP algorithm. The factor graph is shown in fig. 1.

1) i and j denote the indices in $j \in [M] := \{1, 2, ..., M\}$ and $i \in [N] := \{1, 2, ..., N\}$ respectively.

2) The i, j element of the matrix $\mathbf{A}$ will be indicated as A_{ji}.

3) The elements of the vectors $\mathbf{s}, \mathbf{y}, \mathbf{x}$ are indicated by s_i, y_j, x_i respectively.

4) The factor graph $G = (V, F, E)$ has variable nodes $V := [N]$, measurement node $F := [M]$ and edges $E := V \times F = \{(i, j) : i \in [N], j \in [M]\}$. Hence G is the complete bipartite graph with N variable nodes and M measurement nodes. And the messages associated with the edges of this

graph are indicated by Variable to Measurement (VM) message $\{v_{i \to j}\}_{i \in V, j \in F}$, Measurement to

Variable (MV) message $\{\hat{v}_{j \to i}\}_{j \in F, i \in V}$ respectively.
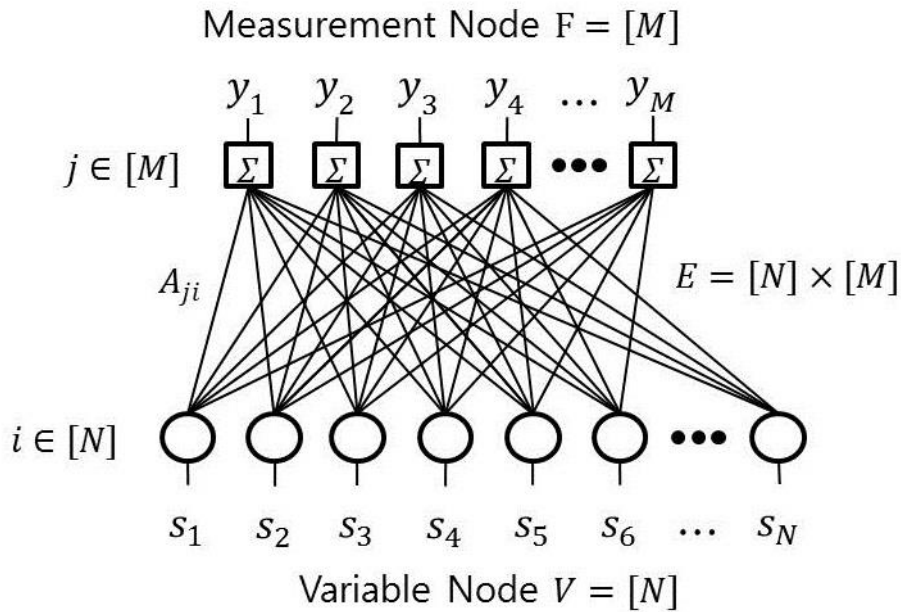
Figure 8 Factor Graph

3.3.2 Applying Classical MP algorithm to CS problem

The first step to derive from classical MP algorithm is to construct Sum-Product algorithm over sparse

signal vector s. For this, when we know sensing matrix $\mathbf{A}$ and measurement vector y, we need

to construct a joint distribution over $\{s_i\}_{i \in [N]}$. And the joint distribution which has several nice

characteristics such as it models well the sparsity in the signal, measurement vector y functions as

factors perfectly with respect to a factor-graph etc. is given below.

$$p(\mathbf{s}) = \frac{1}{C} \prod_{i=1}^{N} \exp(-\beta |s_i|) \prod_{j=1}^{M} \delta(y_j = A_j\mathbf{s}) \tag{19}$$

where C is a normalization constant to make the probability sum equal to unity and $\delta(\cdot)$ denotes a Dirac delta function. There are two distinct components of this distribution; 1) the negative exponential component parameterized with the parameter β. It can be observed that this is a sparsity promoting component whose combined value which is the product of all N factors will get smaller as the signal becomes less sparse i.e. more non-zero values. 2) the Dirac delta function $\delta(\cdot)$ which is only non-zero when the solution satisfies the constraint $y_j = (A\mathbf{s})_j$. Thus the product in equation (19) will assign weights to the solution of the linear system $\mathbf{y} = \mathbf{A}\mathbf{s}$ that will decay exponentially with the $L1$ norm of the solutions. The classical MP algorithm to CS problem can be expressed by table 1 based on equation (19).

Table 1 Classical Message Passing iteration

Algorithm 1   Classical Message Passing iteration
1) Variable to Measurement Message $v_{i \to j}^{t+1}(s_i) = \exp(-\beta |x_i|) \prod_{j' \neq j} \hat{v}_{j' \to i}^{t}(s_i)$ 2) Measurement to Variable Message $\hat{v}_{j \to i}^{t}(s_i) = \int_{\mathbf{x} \backslash x_i} \delta(y_j = A_j\mathbf{s}) \prod_{i' \neq i} v_{i' \to j}^{t}(s_i)$

3.3.3 Transformation from probability distribution form to parameter form of Message

Since the messages are density functions over the real line and the graph is dense, the algorithm 1 is computationally expensive. Fortunately, however, the situation gets simplified when certain

approximation which are valid only in large system limit simplify the MP algorithm without compromising in performance. The approximation in this regard is with respect to the problem associated with classical MP as mentioned above to simplify the messages by assuming they belong to a particular distribution. This makes it possible to track the behavior of these messages as instead of keeping track of all the values of all the probability densities, we will only be required to keep track of the parameters of these representative probability density functions. By the way, we can have question: which parameter can be the message? When N is large, according to the central limit theorem, we can answer this question. Because for large system limit, message can be approximated by Gaussian distribution and we can represent Gaussian distribution from mean and variance.

Let us consider MV message $\hat{v}_{j \to i}$ of Algorithm 1 based on the content we mentioned above. A single MV message $\hat{v}_{j \to i}$ is the probability distribution of the random variable Z in equation (20).

$$Z := y_j - \sum_{i' \neq i} A_{ji'} x_{i' \to j}^t \tag{20}$$

Thus, As equation (20), the probability distribution of Z is decided by random variables $s_1, s_2, \cdots, s_{i-1}, s_{i+1}, s_N$. When N is large and sensing matrix is dense, according to the central limit theorem, Z will be normally distributed with mean and variance approximately. Thus, MV message $\hat{v}_{j \to i}$ is superseded by mean and variance of Z. By the way, the probability distribution of vary according to the measurement node j and iteration index t. Applied this fact, when we let mean and variance of s_i are $x_{i \to j}^t$ and $\hat{\tau}_{i \to j}^t / \beta$, the mean and variance of Z is expressed as given below.

$$z_{j \to i}^t := E(Z) = y_j - \sum_{i' \neq i} A_{ji'} x_{i' \to j}^t \tag{21}$$

$$Var(Z) = Var(A_{ji'}x_{i'}) = \sum_{i' \neq i}(A_{ji'})^2 Var(x_{i'}) = \sum_{i' \neq i}(A_{ji'})^2 \frac{\hat{\tau}^t_{i' \to j}}{\beta} \tag{22}$$

$$\tau_{j \to i} := \sum_{i' \neq i}(A_{ji'})^2 \hat{\tau}^t_{i' \to j} \tag{23}$$

where t is iteration index of algorithm.

Next, we consider about VM message $v_{i \to j}$. As Algorithm 1 in Table 1, VM message is a product of Laplace distribution and $\prod_{j' \neq j}\hat{v}_{j' \to i}$ which is belong to Gaussian distribution. This is because $\prod_{j' \neq j}\hat{v}_{j' \to i}$ is formed from a product of $M-1$ MV messages, all of which are Gaussian distribution. The product of all these Gaussian distribution will be a distribution similar to another Gaussian distribution with modified mean and variance. Summarized this fact, the VM message $v_{i \to j}$ is expressed as the product of a Laplace and Gaussian distribution which is given as follows.

$$f_\beta(s;a,b) := \frac{1}{z_\beta(a,b)} \exp\left\{-\beta|s| - \frac{\beta}{2b}(s-a)^2\right\} \tag{24}$$

where $z_\beta(a,b)$ is normalization constant and such product distribution for a random variable s varies according to parameter a and b. To express VM message $v_{i \to j}$ exactly, we need to decide parameter a and b. If we calculate the equation $\prod_{j' \neq j}\hat{v}_{j' \to i}$, we can get $a = \sum_{j' \neq j}A_{j'i}z^t_{j' \to i}$ and $b = \tau^t_{j \to i}$ [25]. Thus, the distribution of VM message $v_{i \to j}$ is given as below.

$$v^{t+1}_{i \to j} = f_\beta\left(s_i \; ; \; \sum_{j' \neq j}A_{j'i}z^t_{j' \to i} \; , \; \tau^t_{j \to i}\right) \tag{25}$$

Now, we concentrate to calculate mean and variance that will be used as parameter messages. To express mean and variance of VM message $v_{i \to j}$ briefly, we define the mean and variance of $f_\beta(s_i ; a,b)$.

$$F_\beta(a ; b) := E_{f_\beta(s;a,b)}(Z) \tag{26}$$

$$G_\beta(a ; b) := Var_{f_\beta(s;a,b)}(Z) \tag{27}$$

Using Equation (26) and (27), mean $x_{i \to j}^{t+1}$ and variance $\hat{\tau}_{i \to j}^{t}$ of the VM message $v_{i \to j}$ is equal to below.

$$x_{i \to j}^{t+1} = F_\beta \left(\sum_{j' \neq j} A_{j'i} z_{j' \to i}^{t} ; \tau_{j \to i}^{t} \right) \tag{28}$$

$$\hat{\tau}_{i \to j}^{t} = \beta G_\beta \left(\sum_{j' \neq j} A_{j'i} z_{j' \to i}^{t} ; \tau_{j \to i}^{t} \right) \tag{29}$$

Now that we have approximated both types of message which are MV message and VM message of Sum-Product algorithm with distributions having good analytical expressions giving their dependence on some parameters, we only need to track these parameters of the concerned distributions in order to track the behavior of these distributions in different iterations. Luckily, equation (28), (29) give the explicit relationship on how the means and variances of the incoming VM messages at the measurement node are used to update the means and variances of the outgoing MV messages. Thus, we only need to pass the means and variances of messages in both directions. Meanwhile if we observe the variance of MV message as given by equation (23). We observe that due to the presence of a very small element A_{ji} of sensing matrix, we can say the effect of excepted

one message $\left(A_{ji}\right)^2 \hat{\tau}_{i'\to j}^t$ from $\sum_{i'\neq i}(A_{ji'})^2 \hat{\tau}_{i'\to j}^t$ is inadequate. In other word, we can assume the

variance of MV message and VM message to be edge-independent i.e.

$$\tau_{j\to i}^t = \tau^t \qquad \forall i, j \tag{30}$$

Thus τ^t is the value which is updated each iteration without exchanging messages. This value can be obtained by following equation.

$$\tau^{t+1} = \sum_{i'=i}\left(A_{ji'}\right)^2 \beta G_\beta\left(\sum_{j'\neq j} A_{j'i} z_{j'\to i}^t \; ; \; \tau^t\right) \tag{31}$$

And from the distribution of A_{ji}, $E\left(A_{ji}^2\right)$ is $1/M$. Hence equation (31) is approximated by following equation.

$$\tau^{t+1} = \frac{\beta}{M}\sum_i^N G_\beta\left(\sum_j^M A_{ji} z_{j\to i}^t \; ; \; \tau^t\right) \tag{32}$$

3.3.4 Simplification of Message using $\beta \to \infty$

The case when we use a very high value of β or the limit $\beta \to \infty$ in equation (19) is in this case the mass of the prior distribution concentrates narrowly around solutions. It coincides with l_1 norm solution which is with maximum sparsity. Hence, $\beta \to \infty$ limit makes the distribution more pronounced, making it easier to capture it correctly. Interestingly, the case of $\beta \to \infty$ also helps us simplify the F_β and G_β as given (26), (27).

First, we will consider mean F_β of equation (28) in the case of $\beta \to \infty$. The F_β is led by the

integrated term or the maximum value of exponent of the exponential i.e. this is expressed as below.

$$
\begin{aligned}
F_\beta(a,b) &= \int_{-\infty}^{\infty} s f_\beta(s\ ;a,b) ds \\
&= \int_{-\infty}^{\infty} s \frac{1}{z_\beta(a,b)} \exp\left\{-\beta|s| - \frac{\beta}{2b}(s-a)^2\right\} ds \\
&\approx \arg\min{}_s \left\{|s| + \frac{1}{2b}(s-a)^2\right\}
\end{aligned}
\tag{33}
$$

where the minimum value of equation $|s| + \frac{1}{2b}(s-a)^2$ is a point of derivative of the this equation

by variable s. This is equal to below equation.

$$
\begin{aligned}
&\frac{d}{ds}\left\{|s| + \frac{1}{2b}(s-a)^2\right\} = 0 \\
&\frac{1}{b}(s-a) + \mathrm{sgn}(s) = 0
\end{aligned}
\tag{34}
$$

And it is described as Figure 9.
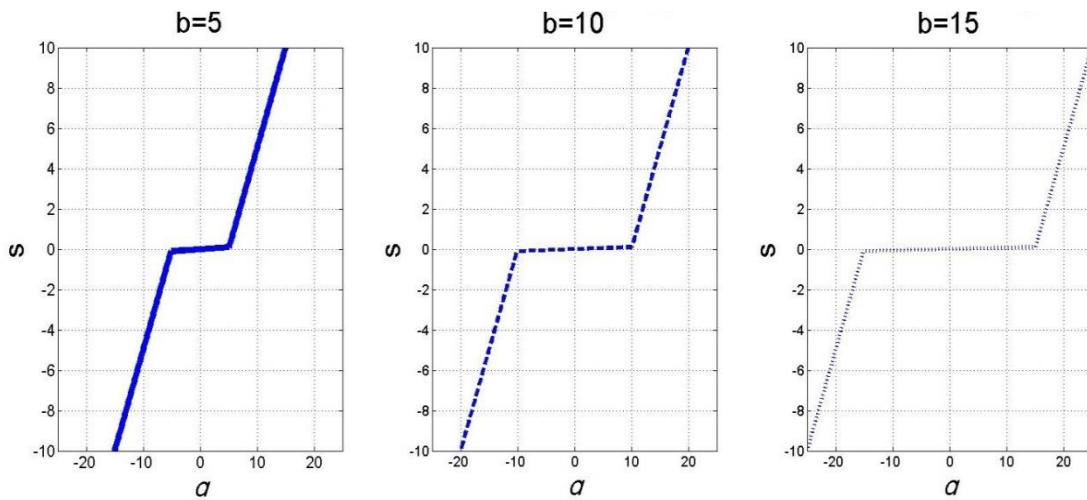
Figure 9 $\operatorname{argmin}_s \left\{ |s| + \dfrac{1}{2b}(s-a)^2 \right\}$ **according to variable** a **and** b

By the way, this corresponds with soft threshold function where x is variable and θ is the threshold value. It is defined as follows.

$$\eta(x;\theta) = \begin{cases} x - \theta & \text{if } x > \theta \\ 0 & \text{if } -\theta \le x \le \theta \\ x + \theta & \text{if } x < -\theta \end{cases} \tag{35}$$

Hence the VM message $v_{i \to j}$ is expressed using soft threshold function briefly as below.

$$x_{i \to j}^{t+1} = \eta \left(\sum_{j' \ne j} A_{j'i} z_{j' \to i}^t \; ; \; \tau^t \right) \tag{36}$$

Figure 10 $\eta'(a \, ; \mathrm{b})$ **function according to variable** a **and** b

Next let us consider about the variance G_β of equation (29). The variance G_β is changed according to the simplified mean of VM message. This is d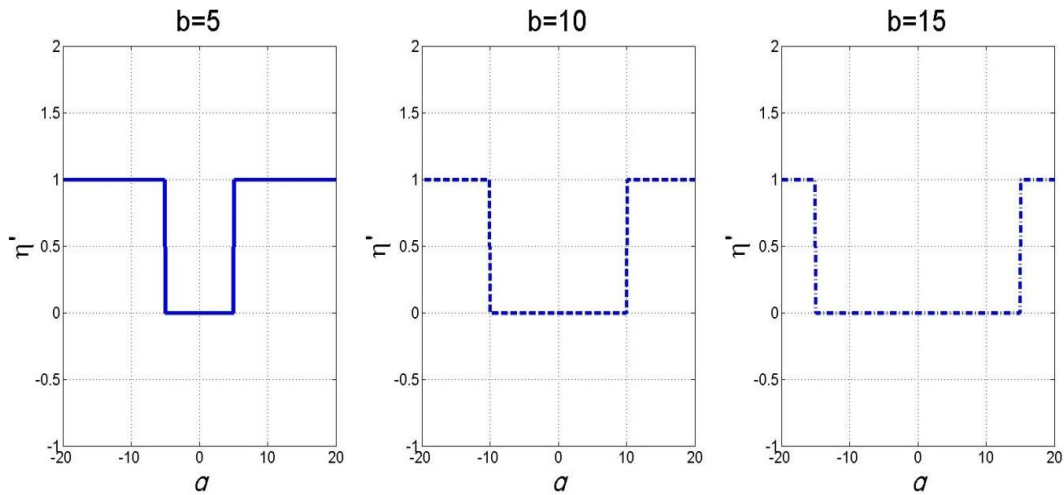ivided into two cases. When the value of the simplified mean is equal to 0, the product distribution can further be approximated as a Laplace distribution. This can be viewed from the perspective that equation (19) is composed of a zero mean Laplace components and a non-zero mean Gaussian distribution. A mean of 0 indicates the primary influence of the Laplace components and hence the product distribution for these cases be approximated as Laplace distribution with variance $2/\beta^2$. In the limit $\beta \to \infty$, this variance can be considered approximately equal to 0. In the another hand, when the value of simplified mean is non-zero, the Gaussian components of equation (19) can be considered to have the primary influence and hence in the limit $\beta \to \infty$, the distribution of equation (19) can be approximated as a Gaussian distribution with variance b/β. Fortunately, both cases can be succinctly expressed in a single expression by using the derivative of the soft threshold function. It is defined as below and described in Figure 10.

$$\eta'(x;\theta) = \begin{cases} 1 & \text{if } -\theta > x > \theta \\ 0 & \text{if } -\theta \le x \le \theta \end{cases} \tag{37}$$

Hence the approximate variance of equation (27) can be written as

$$\lim_{\beta \to \infty} G_\beta(a\ ;b) = \lim_{\beta \to \infty} \frac{b}{\beta}\eta'(a\ ;b) \tag{38}$$

This implies that by using equation (38) in equation (32), the τ^{t+1} can be represented as

$$\tau^{t+1} = \left(\frac{1}{M}\right)\sum_{i}^{N}\hat{\tau}^{t}\eta'\left(\sum_{j}^{M}A_{ji}z_{j\to i}^{t} \; ; \; \tau^{t}\right)$$

$$= \left(\frac{\hat{\tau}^{t}}{N\delta}\right)\sum_{i}^{N}\eta'\left(\sum_{j}^{M}A_{ji}z_{j\to i}^{t} \; ; \; \tau^{t}\right) \tag{39}$$

where δ is M/N.

Until now, we have simplified both the expressions for the mean and variance of equation (28), (32) in the case of $\beta \to \infty$. Thus, we can simplify the parameter-passing MP algorithm by using these simplifications as Algorithm 2.

Table 2 Parameter Passing iteration

Algorithm 2   Parameter Passing iteration
1) Variable to Measurement Message $$x_{i\to j}^{t+1} = \eta\left(\sum_{j'\neq j}A_{j'i}z_{j'\to i}^{t} \; ; \; \tau^{t}\right)$$ 2) Measurement to Variable Message $$z_{j\to i}^{t} = y_{j} - \sum_{i'\neq i}A_{ji'}x_{i'\to j}^{t}$$ 3) Variance Update $$\tau^{t+1} = \left(\frac{\hat{\tau}^{t}}{N\delta}\right)\sum_{i}^{N}\eta'\left(\sum_{j}^{M}A_{ji}z_{j\to i}^{t} \; ; \; \tau^{t}\right)$$

3.3.5 Derivation of AMP from Message Passing algorithm

Although Algorithm 2 is much simplified, it still requires to compute $2MN$ messages in each iteration, which makes the algorithm still computationally expensive when N is large. In this subsection we will the method to reduce the computation cost dramatically.

In order to reduce the computation cost, let us refer Figure 11. Figure 11 (a) describes the MV messages from one measurement node to the entire variable nodes and Figure 11 (b) describes the VM messages from one variable node to the entire measurement nodes. Unlike above algorithm, the messages from one measurement node or variable node to the entire variable nodes or measurement nodes are same regardless of each node. However, due to the message is influenced by each node, we need to add the error correct term $\Delta z^t_{j \to i}$ in the MV message case. Hence we can assume the MV message $z^t_{j \to i}$ is expressed as below.

$$z^t_{j \to i} = z^t_j + \Delta z^t_{j \to i} \tag{40}$$

Likewise, The VM message $x^t_{i \to j}$ also can be expressed as follow.

$$x^t_{i \to j} = x^t_i + \Delta x^t_{i \to j} \tag{41}$$

And then, we will modify Algorithm 2 in table 2 using assumed equations. We substitute equation (41) in the MV message $z^t_{j \to i}$, which results in giving

$$z^t_{j \to i} = \underbrace{y_j - \sum_{i'=1}^{N} A_{ji'} x^t_{i'} - \sum_{i'=1}^{N} A_{ji'} \Delta x^t_{i' \to j}}_{z^t_j} + \underbrace{A_{ji} x^t_i}_{\Delta z^t_{j \to i}} \tag{42}$$

Next, We substitute equation (40) in the VM message $z^t_{j \to i}$, which results in giving

$$x^{t+1}_{i \to j} = \eta \left(\sum_{j'=1}^{M} A_{j'i} z^t_{j'} + \sum_{j'=1}^{M} A_{j'i} \Delta z^t_{j' \to i} - A_{ji} z^t_j \; ; \; \tau^t \right) \tag{43}$$

-33-

We apply the first order Taylor series approximation for the soft threshold function in equation (43).

First order Taylor approximation for a function $f(x)$ is calculated as follows at a specific point a
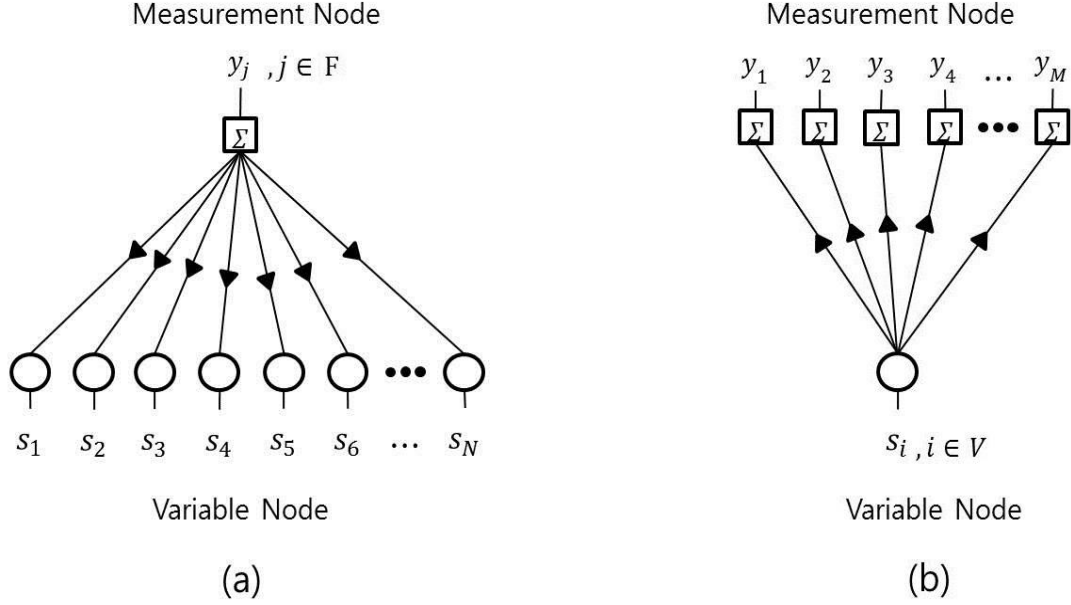

Figure 11 (a) Factor graph describing Measurement to Variable (MV) messages (b) Factor graph describing Variable to Measurement (VM) messages

$$f(x) \approx f(a) + f'(a)(x-a) \qquad (44)$$

where $f'(x)$ indicates the first derivative of $f(x)$. Taylor approximation for the soft threshold function in equation (44) is done at the point which will be common for all the variable nodes. Thus we will have $a = \sum_{j'=1}^{M} A_{j'i} z_{j'}^{t} + \sum_{j'=1}^{M} A_{j'i} \Delta z_{j' \to i}^{t}$. This implies equation (43), the result is below.

$$x_{i \to j}^{t+1} = \underbrace{\eta \left(\sum_{j'=1}^{M} A_{j'i} z_{j'}^{t} + \sum_{j'=1}^{M} A_{j'i} \Delta z_{j' \to i}^{t} \; ; \; \tau^t \right)}_{x_i^t} - \underbrace{A_{ji} z_j^t \eta' \left(\sum_{j'=1}^{M} A_{j'i} z_{j'}^{t} + \sum_{j'=1}^{M} A_{j'i} \Delta z_{j' \to i}^{t} \; ; \; \tau^t \right)}_{\Delta x_{i \to j}^t} \qquad (45)$$

Putting the value of the $\Delta z^t_{j\to i} = A_{ji} x^t_i$ in equation (42) to x^t_i in equation (45), we get the following

$$
\begin{aligned}
x^{t+1}_i &= \eta\left(\sum_{j'=1}^{M} A_{j'i} z^t_{j'} + \sum_{j'=1}^{M} A_{j'i} \Delta z^t_{j'\to i} \; ; \; \tau^t \right) \\
&= \eta\left(\sum_{j'=1}^{M} A_{j'i} z^t_{j'} + \sum_{j'=1}^{M} A_{j'i} (A_{j'i} x^t_i) \; ; \; \tau^t \right) \\
&= \eta\left(\sum_{j'=1}^{M} A_{j'i} z^t_{j'} + x^t_i \; ; \; \tau^t \right)
\end{aligned}
\tag{46}
$$

Likewise putting the value of the $\Delta x^t_{i\to j}$ in equation (45) to z^t_j, we get the following

$$
\begin{aligned}
z^t_j &= y_j - \sum_{i'=1}^{N} A_{ji'} x^t_{i'} - \sum_{i'=1}^{N} A_{ji'} \Delta x^t_{i'\to j} \\
&= y_j - \sum_{i'=1}^{N} A_{ji'} x^t_{i'} + \sum_{i'=1}^{N} A^2_{ji'} z^{t-1}_j \eta'\left(\sum_{j'=1}^{M} A_{j'i} z^t_{j'} + \sum_{j'=1}^{M} A_{j'i} \Delta z^t_{j'\to i'} \; ; \; \tau^t \right) \\
&= y_j - \sum_{i'=1}^{N} A_{ji'} x^t_{i'} + \frac{z^{t-1}_j}{M} \sum_{i'=1}^{N} \eta'\left(\sum_{j'=1}^{M} A_{j'i} z^t_{j'} + x^{t-1}_i \; ; \; \tau^t \right) \\
&= y_j - \sum_{i'=1}^{N} A_{ji'} x^t_{i'} + \underbrace{\frac{z^{t-1}_j}{\delta} \left\langle \eta'\left(\sum_{j'=1}^{M} A_{j'i} z^t_{j'} + x^{t-1}_i \; ; \; \tau^t \right) \right\rangle}_{\text{Onsager Term}}
\end{aligned}
\tag{47}
$$

where $\delta = \dfrac{M}{N}$, $\langle \cdot \rangle = \dfrac{\sum_{i=1}^{N}(\cdot)}{N}$.

Thus, the final AMP algorithm can be represented as Algorithm 3 in table 3.

Table 3 AMP iteration

Algorithm 3   AMP iteration
1)   Variable to Measurement Message

$$\mathbf{x}^{t+1} = \eta\left(\mathbf{A}^{T}\mathbf{z}^{t} + \mathbf{x}^{t} \ ; \ \tau^{t}\right)$$

2) Measurement to Variable Message

$$\mathbf{z}^{t} = \mathbf{y} - \mathbf{A}\mathbf{x}^{t} + \underbrace{\frac{\mathbf{z}^{t-1}}{\delta}\left\langle\eta'\left(\mathbf{A}^{T}\mathbf{z}^{t-1} + \mathbf{x}^{t-1} \ ; \ \tau^{t}\right)\right\rangle}_{\text{Onsager Term}}$$

3) Variance Update

$$\tau^{t+1} = \frac{\tau^{t}}{\delta}\left\langle\eta'\left(\mathbf{A}^{T}\mathbf{z}^{t} + \mathbf{x}^{t+1} \ ; \ \tau^{t}\right)\right\rangle$$

4　Compressive sensing in UWB communication

4.1　Problem Statement

The recent steady growth in technology and the commercial deployment of wireless communication are considerable affecting our daily lives. And the transition from analog to digital communications are enabling consumers to access a wide range of information from anywhere and at any time. In wireless communication networks a rapid increase in demand for higher capacity, faster service, and more secure wireless communication are observed. Hence, new advanced technologies are required to achieve this problem in overcrowded spectrum.

UWB (Ultra-wideband) technology offers an expectable solution to the spectrum exhaustion by allowing new services to coexist with current radio systems with minimal or no interference [14]. In UWB communications, an ultra-short duration pulse, typically on the order of nanoseconds, is used as the elementary pulse-shaping to carry information [15]. Transmitting very short pulses leads to several desirable characteristics. Firstly, the large bandwidth for UWB pulses is improved channel capacity. And UWB communications systems are capable of working in communication channel with low SNR. Secondly, UWB communication systems have immunity to detection and intercept. Because detecting very short pulses without knowing when they will arrive is next to impossible. Thirdly, the very short duration of UWB pulses makes less sensitive to the multipath effect. Because the transmission duration of a UWB pulse is shorter than a nanosencond in most case, the reflected pulse has an extremely short window of opportunity to collide with reflected pulses. Finally, UWB transmission is carrierless, meaning that data is not modulated on a specific carrier frequency. For this reason UWB transceiver architecture is significantly simpler and cheaper to build [16].

However, there are many challenges including pulse shape distortion, channel estimation, time synchronization and so on using UWB communications [17]. Most of all, the extremely high

bandwidth of the received UWB signal requires high speed analog to digital converters (ADC). These speeds demand the use of a bank of polyphase ADC with accurate timing control [18]. However this system has low resolution in comparison with consuming a lot of power and incurs high circuit complexity. Furthermore, oversampling of the received UWB signal may be required to improve channel estimation. Such daunting sampling rates are not practicable with the latest ADC technology. New methods for UWB channel estimation are needed to accomplish the required sampling rates.

4.2   UWB Channel estimation based on Compressive Sensing

To solve the problem mentioned above, we propose to use a compressive sensing framework. Compressive sensing is a new concept based on the theoretical results of signal reconstruction with random basis coefficients. A signal with a large number of data point that is sparse in some basis matrix $\mathbf{T}$, can be exactly reconstructed using only a few number of random projections of the signal onto a random matrix $\mathbf{A}$ that is incoherent with $\mathbf{T}$. In general, the number of projections is much smaller than the number of samples in the original signal. Hence, we can reduce the sampling rate and use reduced ADC resources [2].

Consider the simple communications model of transmitting a pulse $p(t)$ throughout a noiseless UWB communication channel $h(t)$. The received UWB signal can be modeled as

$$r(t) = p(t) * h(t) = \sum_{l=0}^{L-1} \alpha_l p(t - \tau_l) \tag{48}$$

where $p(t)$ is the very short pulse used to convey information with a time duration in the order of nanoseconds. Typically, a Gaussian pulse or its derivatives are used as the UWB pulses.

In Equation (48), $h(t)$ is the impulse response of the UWB channel and has been modeled as

$$h(t) = \sum_{l=0}^{L-1} \alpha_l \delta(t - \tau_l) \tag{49}$$

where $\delta(\bullet)$ is the dirac delta function, τ_l and α_l are, respectively, the delay and gain associated with the l-th path of the UWB channel and L is the number of propagation paths.

In our analysis, the set of delays and gains are generated according to the models proposed by the IEEE 802.15.4a working group in [19] and we restrict our analysis to real-valued UWB channel models where there is not pulse distortion.

Note in equation (48) that the received UWB signal is composed of scaled and time delayed versions of the transmitted pulse. Note also that the statistics of the arrival paths define the time space between pulses. Thus, if the averaged path inter-arrival time is greater than the pulse duration, the received UWB signal presents less pulse overlapping and therefore more sparsity is expected. On the other hand, for dense multipath UWB channel like NLOS propagation where the multipath components arrive closely spaced, a more pulse-overlapping is found. For this reason, to reconstruct the channel using time sparsity model is not suitable.

CS theory relies on the fact that the underlying signal is sparse in some basis domain, it is important to define a suitable basis matrix $\mathbf{T}$ to represent the received UWB signal. In particular, the transmitted pulse shapes suggest the use of basis representations that can provide a better sparse representation of the received UWB signals.

Since the received UWB signal is formed by results of convolution with transmitted pulse and channel impulse response, the basis matrix $\mathbf{T}$ is generated by shifting the transmitted pulse, i.e. convolution matrix composed of transmitted pulse and let $\mathbf{r}, \mathbf{h}, \mathbf{p}$ be a discrete time representation of the received signal, multipath channel, transmitted pulse respectively. That is, $\mathbf{r} = \left[r(0), r(T), \cdots r((L-1)T) \right]^\dagger$, $\mathbf{h} = \left[h(0), h(T), \cdots h((N-1)T) \right]^\dagger$, $\mathbf{p} = \left[p(0), p(T), \cdots p((P-1)T) \right]^\dagger$ where T is the sampling

period, L, N, P is the number of samples and † denotes the transpose operator. Then, the received signal (48) can be represented by below.

$$\mathbf{r} = \begin{bmatrix} r(0) \\ r(T) \\ r(2T) \\ \vdots \\ r((L-1)T) \end{bmatrix} = \mathbf{Th}$$

$$= \begin{bmatrix} p(0) & 0 & \cdots & 0 & 0 \\ p(T) & p(0) & \cdots & \vdots & \vdots \\ p(2T) & p(T) & \cdots & 0 & 0 \\ \vdots & p(2T) & \cdots & p(0) & 0 \\ p((P-2)T) & \vdots & \cdots & p(T) & p(0) \\ p((P-1)T) & p((P-2)T) & \vdots & \vdots & p(T) \\ 0 & p((P-1)T) & \cdots & p((P-3)T) & \vdots \\ 0 & 0 & \cdots & p((P-2)T) & p((P-3)T) \\ \vdots & \vdots & \vdots & p((P-1)T) & p((P-2)T) \\ 0 & 0 & 0 & \cdots & p((P-1)T) \end{bmatrix} \times$$

$$\begin{bmatrix} h(0) \\ h(T) \\ h(2T) \\ \vdots \\ h((N-1)T) \end{bmatrix} \tag{50}$$

Furthermore, let $\mathbf{y} = \mathbf{Ar}$ be the random projected signal where $\mathbf{A}$ is the measurement matrix with a row vector with pseudo-random (PN) Bernoulli sequence. The AMP algorithm is then applied on the random projected signal $\mathbf{y}$ and the $\mathbf{F}$ that is product of $\mathbf{A}$ and $\mathbf{T}$. Finally, the AMP algorithm outputs a sparse vector $\mathbf{h}$ that is a discrete time representation of multipath channel. The proposed system is shown in Figure 12.
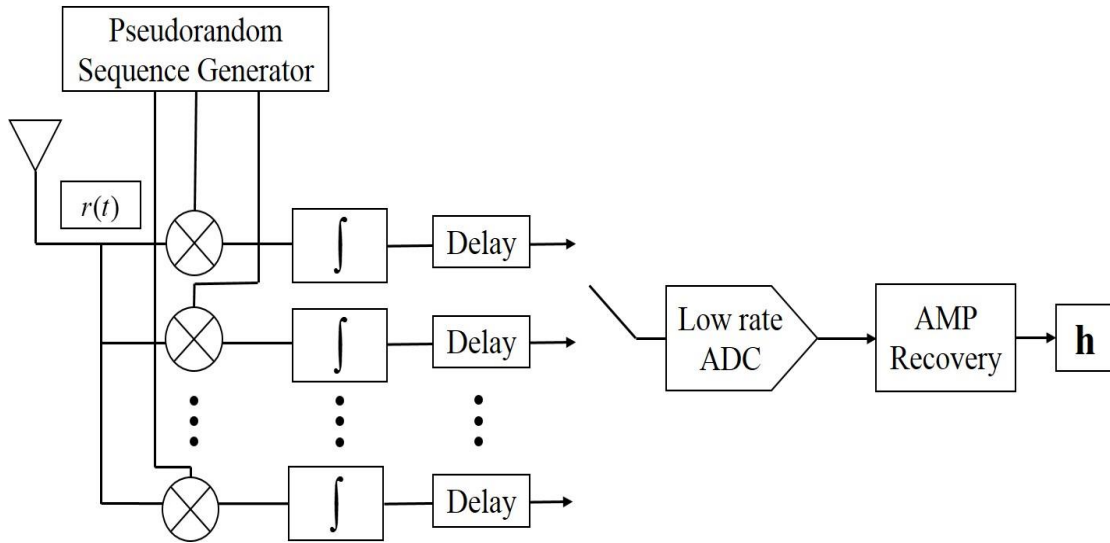
Figure 12 The channel estimation system based on Compressive Sensing

4.3   RAKE receiver using channel estimation based on Compressive Sensing

According to Equation (48), different replicas of the same transmitted pulse overlap at the receiver

only when the corresponding inter-arrival time is smaller than pulse duration T_M . In this case, signals

associated with different paths are not independent, that is, the amplitude of the pulse observed at

time t is affected by the presence of multipath contributions arriving immediately before or after

time t . Given the characteristics of the propagation channel, the number of independent paths at the

receiver depends on T_M . The smaller T_M , the higher the number of independent contributions at the

receiver input. For UWB systems, the T_M value is on the order of nanoseconds or fractions of

nanoseconds, leading to the hypothesis that all multipath contributions are non-overlapping, so that

the received waveform consists of several independent components. UWB systems can thus in

principle take advantage of multipath propagation by combining a large number of different and

independent replicas of the same transmitted pulse.

Different strategies for exploiting diversity can be adopted by the receiver: Selection Diversity (SD),

Equal Gain Combining (EGC), and Maximal Ratio Combining (MRC). With the method, the receiver

selects the multipath contribution exhibiting the best signal quality and operates the decision on the observation of the contribution only. Choosing the best path guarantees an increase in receiver performance with respect to the simple selection of the first path, deriving from having selected the path with highest instantaneous SNR. A different method for increasing SNR consists of combining multi path contributions rather than selecting the best path. With the EGC method in particular, the different contributions are first aligned in time and then added without any particular weighting. In MRC, the different contributions are weighted before the combination and the weights are determined to maximize the SNR before the decision process. In the presence of Gaussian noise at the receiver, the SNR is maximized by applying to each multi-path contribution a weighting factor that is proportional to the amplitude of the corresponding received signal. In other words, the MRC method adjusts the received contributions before combining them. The adjustment is performed by amplifying the strongest components and by attenuating the weak ones. In a single-user communication system without ISI, the method that achieves the best performance is the MRC, which ensures the largest SNR at the combiner output.

In all the above cases, the receiver takes advantage of multi-path under the hypothesis that different replicas of the same transmitted pulse can be analyzed separately and eventually combined before decision. The optimum correlator for the present case must include additional correlators associated with different replicas of a same transmitted waveform. Such a scheme is called the RAKE receiver.

Figure 13 shows the structure of the RAKE receiver, which consists of a parallel bank of N correlators, followed by a combiner that determines the variable to be used for the decision on the transmitted symbol. Each correlator is locked on one of the different replicas of the transmitted symbol, that is, the correlator mask $m_j(t)$ on the j-th branch of the RAKE is aligned in time with the j-th delayed replica of the transmitted symbol.
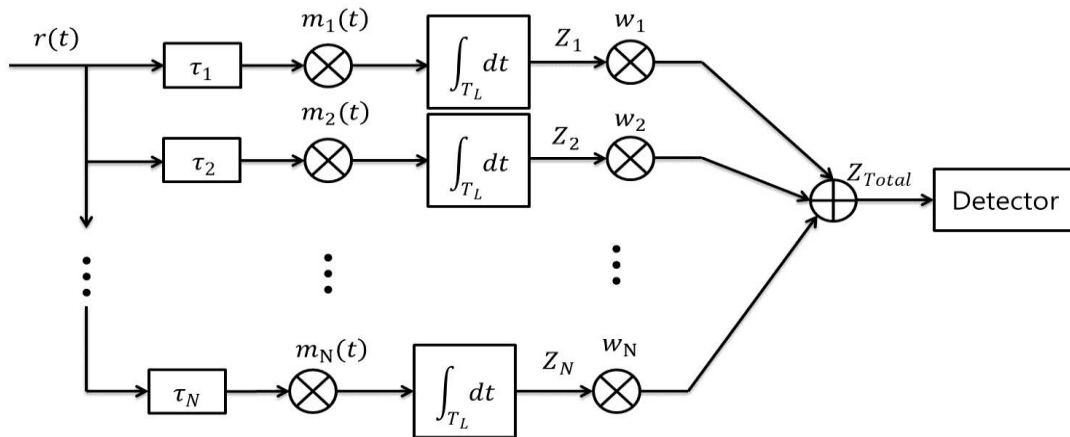
Figure 13 RAKE receiver with N parallel correlators

The output of the bank of correlators feeds the combiner. Depending on the diversity method implemented at the receiver, a different set of weighting factors $\{w_1, \cdots, w_N\}$ is used to combine the outputs of the correlators. In the MRC case, the output of each branch is multiplied by a weighting factor, which is proportional to the signal amplitude on that branch.

According to the schemes of Figure 13, the RAKE receiver must know the time distribution for all multi-path contributions composing the received waveform. This task is performed by supplying the RAKE with the capability of scanning the channel impulse response, tracking, and adjusting the delay of a certain number of multi-path components. Time delay synchronization for the different multi-path contributions is based in general on correlation measurements that are performed on the received waveform. In addition, MRC methods are adopted the knowledge of the amplitudes of the multi-path components. This calls for an extension of the channel estimation based on Compressive Sensing described above. The proposed RAKE receiver is shown Figure 14.
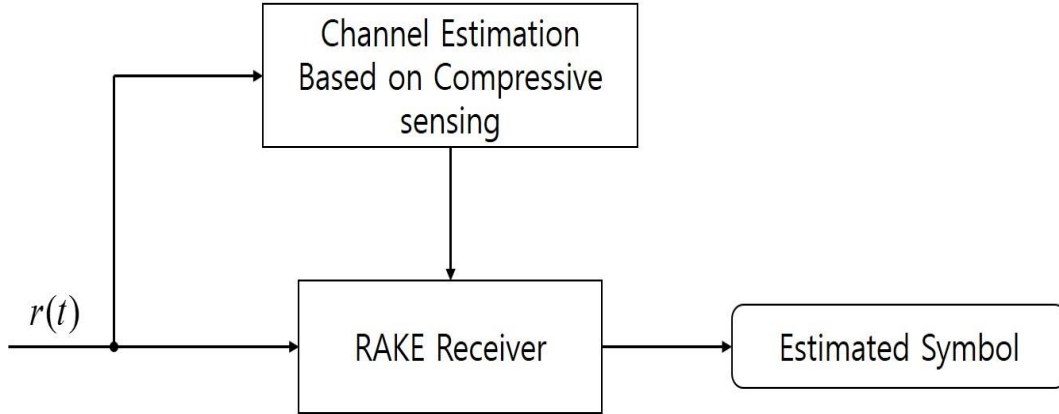
Figure 14 RAKE receiver using channel estimation based on Compressive Sensing

4.4   Numerical Simulation

In this section, we show the performance of the proposed UWB channel estimation by changing the recovery algorithm. All the UWB communication environments and propagation scenarios proposed by the IEEE 802.154.4a in [19] are used as channel models.

We select the second derivative of the Gaussian pulse as the transmitted pulse waveform that has been normalized to have unit energy and a pulse duration of 0.5ns. Further, the transmitted parameters are set to T_f is 40ns and the number of frame is 100. The sampling frequency before the projection stage in all the simulation was 20 GHz, which is higher than the Nyquist rate.

The UWB multipath channel has been simulated following the parameterized model proposed by the IEEE 802.15.4a working group. For the sake of simplicity in our simulation, UWB channels has real valued impulse responses. Furthermore, the multipath impulse response are cut off to make the maximum delay spread of the multipath channel equal to 99.35ns.

4.4.1 Compare with existing estimation method [21] and CS method

First of all, if the proposed channel estimation method cannot achieve similar performance with existing UWB channel estimation method, it will be useless. Thus, we compared with existing UWB

channel estimation method. In this simulation, four types of standard IEEE 802.14.3a channel models [22] are used and the performance is evaluate by normalize MSE that equal to following equation.

$$NMSE = 10 \times \log_{10} \left(\frac{MSE}{MSE \text{ at } -10\text{dB}} \right) \qquad (51)$$

Left of Right of Figure 15 show performance of existing UWB channel estimation and proposed estimation method respectively. As you can see, the channel estimation improves according to SNR increases both figures. However, the improvement rate from proposed one is a little bit higher than existing one. Thus, proposed one can not only reduce sampling rate and but also improve channel estimation performance.
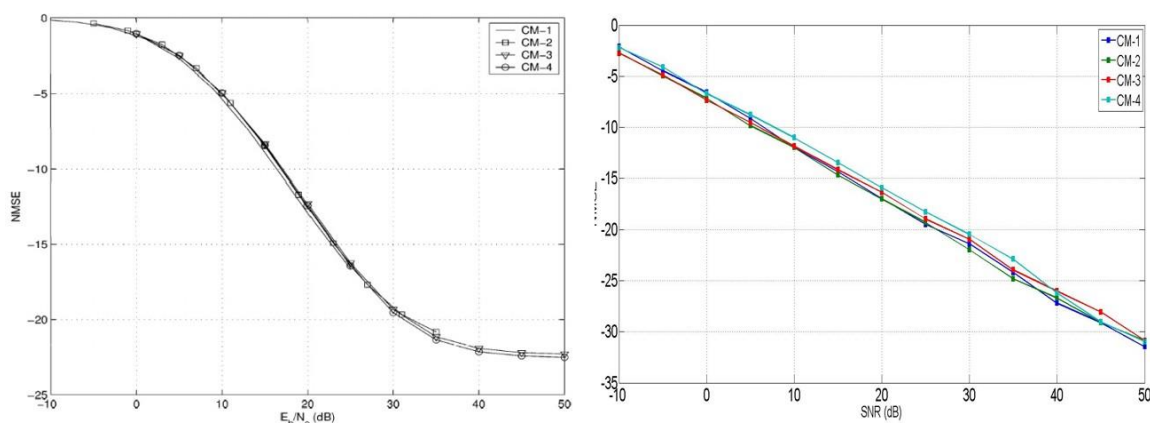

Figure 15 (a) Existing estimation method [21] (b) Proposed CS estimation method (20% of Nyquist rate)

4.4.2 Phase transition for different recovery algorithm

It is very convenient to display results graphically with a set of undersampling, sparsity coordinates :

$\delta = M / N$ and $\rho = k / M$. The δ measures the degree of determinacy or indeterminacy of the

system and The ρ measures the sparsity or density of the channel to be estimated. ρ close to zero means the channel vector is very sparse, and ρ close to 1 means it is almost fully dense. We call the domain $(\delta, \rho) \in [0,1]^2$ is phase space.

Figure 16 depicts the phase transition for different recovery algorithms. The curves indicate the fraction of successful reconstruction at (δ, ρ). There are two clear phases. Upper phase is lower than 50% success rate and Lower phase is more than 50% success rate over 20 iterations. The success is decided when the MSE of estimated channel exceeded 0.999, i.e. when $MSE < 0.001$.
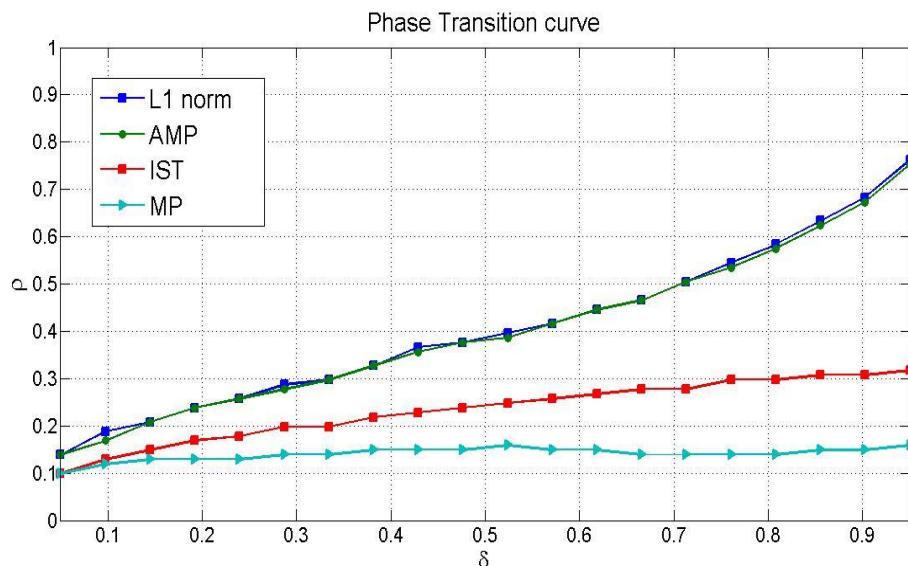

Figure 16 Observed Phase Transition for different recovery algorithms ; AMP, Iterative Soft Thresholding (IST), L1 norm, Matching Pursuit (MP)

We compared with 4 different recovery algorithms; AMP, Iterative Soft Thresholding (IST), L1 norm, Matching Pursuit (MP). This is because, the structure of the AMP algorithm is intimately related to the IST, L1 norm is the standard recovery algorithm for compressive sensing and MP algorithm is already used to estimate channel in [20]. This result shows AMP and L1 norm have wider success phase region. This means the performance of channel estimation used AMP and L1 norm algorithm

is better than MP and IST and it is possible to reconstruct the channel from lower measurements than MP and IST.

4.4.3 Average time on successful reconstruction of channel for different recovery algorithms

Figure 17 depicts the average time on channel estimation for different recovery algorithms. In this simulations, the UWB communication channel is modeled as an indoor residential environment, the number of measurement is 20% of samples.

Estimating the channel is computationally expensive and is not suitable for real time applications. Thus, faster recovery algorithms is needed to apply to UWB channel estimation. According to result, AMP and MP are computationally simple and suitable for UWB channel estimation.
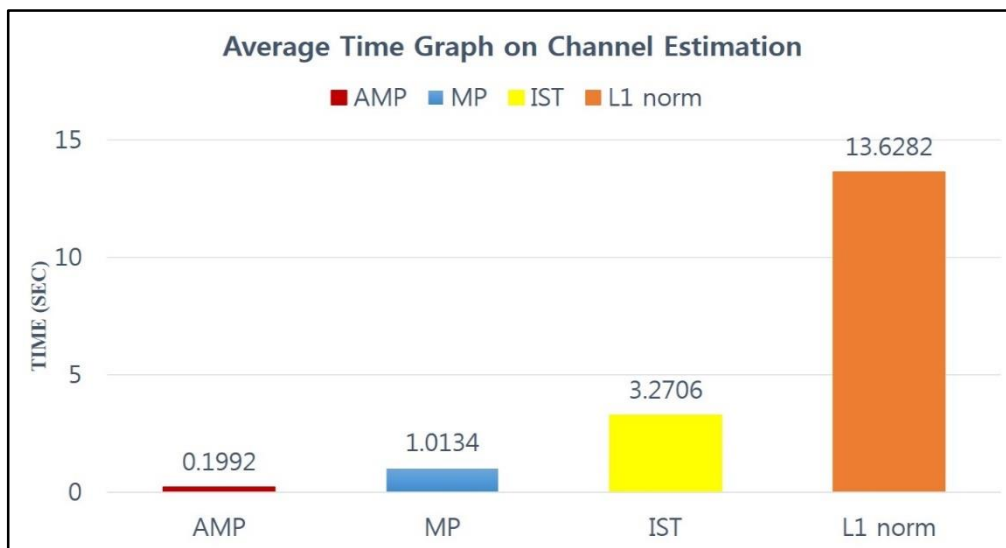

Figure 17 Average Time Graph on Channel Estimation for different recovery algorithms

4.4.4 BER performance of RAKE receiver for different recovery algorithms

The BER curve shown Figure 18 are depicted as a function of signal-to-noise (SNR) ratio. In this simulations, the UWB channel is modeled as an indoor residential environment, the number of measurements is 20% of the samples. The number of finger for RAKE is set to 20.

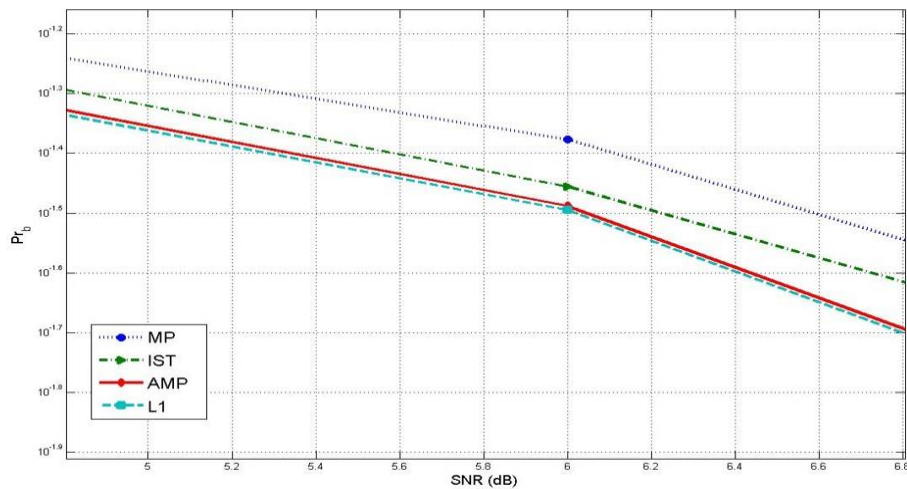As it can be seen from Figure 10, the RAKE receiver used AMP and L1 norm outperforms for all range of SNR.

Figure 18 Indoor residential BER performance of RAKE receiver for different recovery algorithms

4.4.5 BER performance for different sampling rate

Figure 19 shows the BER performance of RAKE receiver used AMP for different sampling rate. For comparative purposes, the BER performance for the ideal RAKE receiver is also shown in Figure 19. As expected, the performance of RAKE receiver used AMP improves as the sampling rate increases. More interesting, RAKE receiver used AMP achieves the same performance than that yielded by the ideal RAKE receiver from only 30% of channel's samples.
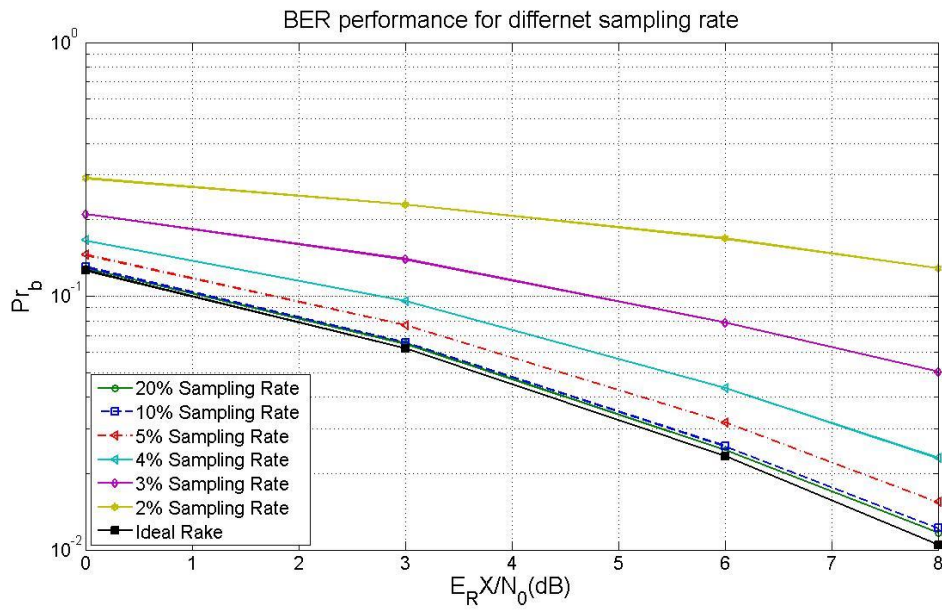
Figure 19 BER performance for different sampling rate

5 Conclusion

In this paper, we have introduced AMP algorithm for compressive sensing signal recovery and applied to the channel estimation for wireless UWB communications. We have provided not only an understanding of the AMP algorithm but also its relationship with a classical Message Passing algorithm. And we also have shown the possibility to reconstruct channel from a reduced number of random projections of the received UWB signal. Numerical results show that AMP is faster and more efficient recovery algorithm. Thus, the AMP is suitable for UWB channel estimation.

In this paper, the theory of compressive sensing and AMP algorithm for compressive sensed signal recovery have been used for UWB channel estimation. UWB channel estimation is one of applications that Compressive sensing and AMP can be applied. We assure these theories can be extended to a much broader range of applications in wireless communications due to advantage of reducing sampling rate.

REFERENCES

[1] Heung-No Lee "Lecture note: Introduction to compressed sensing with coding theoric perspective", Spring, 2011.

[2] David Donoho, "Compressed sensing," IEEE Trans. On Information Theory, 52(4), pp.1289-1306, April, 2006.

[3] D. L. Donoho, A. Maleki, "Message passing algorithms for compressed sensing: I. motivation and construction," Proc. of Information Theory Workshop(ITW), 2010 IEEE, pp. 1-5, Cairo Egypt, Jan. 2010.

[4] M. Bayati and A. Montanari, "The dynamics of message passing on dense graphs, with applications tocompressed sensing," IEEE Transactions on Information Theory, vol. 57, no. 2, pp. 764–785, Feb. 2011.

[5] D. L. Donoho, A. Maleki, and A. Montanari, "Message passing algorithms for compressed sensing," Proc. National Academy of Sciences, vol. 106, no. 45, pp. 18914–18915, 2009.

[6] I. Daubechies, M. Defrise, C. De Mol "An iterative thresholding algorithm for linear inverse problems with a sparsity constraint" Comm. Pure Appl. Math., 57 (11) (2004), pp. 1413–1457

[7] S. Mallat and Z. Zhang, "Matching pursuits with time-frequency dictionaries," IEEE Trans. Signal Process., vol. 41, pp. 3397–3415, Dec.1993.

[8] Emmanuel Candes, Justin Romberg, and Terence Tao, "Robust uncertainty principles: Exact signal reconstruction from highly incomplete frequency information," IEEE Trans. On Information Theory, 52(2) pp. 489-509, February, 2006.

[9] Emmanuel Candes and Terence Tao, "Near optimal signal recovery from random projections: Universal encoding strategies," IEEE Trans. On Information Theory, 52(12), pp. 5406-5425 December, 2006.

[10] S.S. Chen, D.L. Donoho, M.A. Saunders, "Atomic decomposition by basis pursuit," SIAM J. Sci. Comput., Vol.20, No.1, pp.33-61, 1998.

[11] D.L. Donoho and X. Huo, "Uncertainty principles and ideal atomic decomposition," IEEE Trans. Information Theory, Vol.47, pp.2845-2862, Nov., 2001.

[12] F.R. Kschischang, B.J. Frey and H.A. Loeliger, "Factor Graphs and the Sum-Product Algorithm" IEEE Transactions on Information Theory, vol. 47, pp. 498-519, Feb 2001.

[13] D. L. Donoho, Y. Tsaig, I. Drori, J. L. Starck ," Sparse Solution of Underdetermined Systems of Linear Equations by Stagewise Orthogonal Matching Pursuit ", IEEE Transactions on Information Theory, Vol. 58, No. 2, pp. 1094-1121, February 2012.

[14] R. C. Qiu, H. Liu, and X. Shen, "Ultra-wideband for multiple access communications," IEEE Commun. Mag., vol. 43, no. 2, pp. 80–87, Feb.2005.

[15] J. H. Reed, An Introduction to Ultra Wideband Communication Systems, ser. Prentice Hall Communications Engineering and Emerging Technologies Series, T. S. Rappaport, Ed. Upper Saddle River, NJ:Prentice-Hall, 2005.

[16] V. Lottici, A. D'Andrea, and U. Mengali, "Channel estimation for ultra-wideband communications," IEEE J. Select. Areas Commun.,vol. 20, no. 12, pp. 1638–1645, Dec. 2002.

[17] L. Yang and G. B. Giannakis, "Ultra-wideband communications: An idea whose time has come," IEEE Signal Process. Mag., vol. 21, no. 6, pp. 26–54, Nov. 2004.

[18] O'Donnell, M. Chen, S. Wang, and R. W. Brodersen, "An integrated, low-power, ultra-wideband tranceiver arquitecture for low-rate, indoor wireless system," in IEEE CASWorkshop onWireless Communications and Networking, Sep. 2002.

[19] A. F. Molisch *et al.*, IEEE 802.15.4a channel Model—Final report Tech. Rep. Doc. IEEE 802.15-04-0662-02-004a, 2005

[20] J. L. Paredes, G. R. Arce, and Z. Wang, "Ultra-wideband compressed sensing: Channel estimation," IEEE J. Sel. Topics Signal Proc., vol. 1, no. 3, pp. 383–395, Oct. 2007.

[21] Y. Li, A. F. Molisch, and J. Zhang, "Channel estimation and signal detection for UWB," WPMC, Wireless Personal Multimedia Communications, Oct. 2003.

[22] J. Foerster (editor), "Channel Modeling Sub-committee Report Final," IEEE802.15-02/490.

[23] J. A. Tropp , "Just relax: convex programming methods for identifying sparse signals in noise", IEEE Transactions on Information Theory, Vol. 52, No. 3. pp. 1030-1051, March 2006.

[24] E. Candes, M. Wakin, "An introduction to compressive sampling ", IEEE Signal Processing Magazine, vol. 25 pp. 21–30, 2008.

[25] J. A. Tropp and A. C. Gilbert, "Signal recovery from random measurements via orthogonal matching pursuit," IEEE Transactions on Information Theory, vol. 53, no. 12, pp. 4655.4666, Dec. 2007.

[26] Donoho, D.L. and Tanner. J., "Precise Undersampling Theorems", Proceedings of the IEEE, Vol. 98, pp.913-924, May, 2010.

[27] M. R. Osbome, B. Presnell, and B. A. Turlach, "A new approach to variable selection in least squares problem," IMA J. Numer. Anal., Vol.20, pp. 389-403, 2000.

[28] D. L. Donoho and Taakov Tsaig, "Fast solution of L1-norm Minimization Problems When the Solution May Be Sparse," IEEE Trans on Information Theory, Vol.54, No.11, pp.4789-4812, 2008.

[29] B. Efron, T. Hastle, I. M. Johnstone, and R. Tibshirani, "Least angle regression," Ann. Statist., Vol.32, No.2, pp.407-499, 2004.

[30] Rober Tibshirani, "Regression Shrinkage and Selection via the LASSO," Journal of the Royal Selection via the LASSO," Journal of the Royal Statistical Society. Series B (Methodological), Vol.58, Issue 1, pp.267-288, 1996.

[31] E. Candes, J. Romberg, and T. Tao, "Stable signal recovery from incomplete and inaccurate measurements," Comm. Pure Appl. Math., Vol.59, No.8, pp. 1207-1223, Aug., 2006.

[32] H. H. Baek, S. J. Park, J. M. Ryu and H. N. Lee, "Reanalysis of Approximate Message Passing (AMP) for Compressed Sensing Signal Recovery," in Proc. KICS Int. Conf. Commun. 2013 (KICS ICC 2013), pp. 701-702 Jeju Island, Korea, June 2013.

[33] Jaewook Kang, Heung-No Lee, and Kiseon Kim, "Bayesian hypothesis test using nonparametrix belief propagation for noisy sparse recovery," submitted to IEEE Transactions on Signal Processing.

[34] M. Akcakaya, J. Park, and V. Tarokh, "A coding theory approach to noisy compressive sensing using low density frame," IEEE Transactions on Signal Processing, vol. 59, no. 12, pp. 5369-5379, Nov. 2011.

[35] R. Tibshirani, "Regression shrinkage and selection via the lasso," Journal of the Royal Statistical Society: Series B, vol. 58, no. 1, pp. 267-288, 1996.

[36] A. Maleki and D. L. Donoho, "Optimally tuned iterative reconstruction algorithms for compressed sensing," IEEE Journal of selected topics in signal processing, vol. 4, no 2, Apr. 2010.

[37] D. L. Donoho, A. Maleki, and A. Montanari, "The noise-sensitivity phase transition in compressed sensing," IEEE Transactions on Information Theory, vol. 57, no. 10, pp. 6920-6941, Oct. 2011.

[38] A. Maleki, and D. L. Donoho, "Optimally tuned iterative Reconstruction Algorithms for compressed sensing," IEEE Journal of Selected Topics in Signal Processing, vol. 4, pp. 330-341, Apr. 2010.

ACKNOWLEDGEMENT